Spring 1969

HOT ATOM CHEMISTRY OF PHOSPHORUS-32 IN ALKALI CHLORIDES AND SODIUM SILICATES

MERAL TAYAN ERCAN
University of New Hampshire, Durham

70-2087

ERCAN, Meral Tayan, 1943-
HOT ATOM CHEMISTRY OF ^{32}P IN
ALKALI CHLORIDES AND SODIUM SILICATES.

University of New Hampshire, Ph.D., 1969
Chemistry, radiation

University Microfilms, Inc., Ann Arbor, Michigan

HOT ATOM CHEMISTRY OF ^{32}P IN ALKALI CHLORIDES AND SODIUM SILICATES

BY

MERAL TAYAN ERCAN

B. S., American College for Girls in
Istanbul, Turkey, 1964

A THESIS

Submitted to the University of New Hampshire
In Partial Fulfillment of
The Requirements for the Degree of
Doctor of Philosophy

Graduate School
Department of Chemistry
May, 1969

This thesis has been examined and approved.

Charles W. Owens, Asst. Prof. of Chemistry
Thesis Director

Charles V. Berney, Asst. Prof. of Chemistry

James H. Weber, Asst. Prof. of Chemistry

Helmut M. Haendler, Professor of Chemistry

Richard L. Kaufmann, Assoc. Prof. of Physics

May 23, 1967
Date

ACKNOWLEDGEMENT

This research, supported in part by a grant from the Research Corporation and by a National Science Foundation grant, was performed in the chemistry laboratories of the University of New Hampshire under the direction of Dr. Charles W. Owens.

The author wishes to express her sincere appreciation to Dr. Owens for the encouragement and the assistance so generously given during the development of this thesis.

She wishes to dedicate this thesis to her parents, Hasan and Layika Tayan.

Meral Tayan Ercan

TABLE OF CONTENTS

PART I

TABLE OF CONTENTS

PART II

LIST OF TABLES

PART I

LIST OF TABLES

PART II

LIST OF FIGURES

PART I

LIST OF FIGURES

PART II

ABSTRACT

HOT ATOM CHEMISTRY OF ^{32}P IN
ALKALI CHLORIDES AND SODIUM SILICATES

by

MERAL TAYAN ERCAN

Valence distribution and photo-annealing of ^{32}P produced by $^{35}Cl(n,\alpha)^{32}P$ reaction were studied in the alkali chlorides: lithium, sodium and potassium chloride.

Fisher certified reagent grade alkali chlorides were used without further purification, except that they were annealed at 100°C for two hours to drive off water of absorption. Irradiations of 200 mg quantities of alkali chlorides in vacuum-sealed quartz tubes were carried out at the U. S. Army Materials and Mechanics Research Reactor, Watertown, Mass., at a flux of 2×10^{12} n /cm^2/sec. The irradiation time was 5 minutes. The irradiated samples were kept at room temperature in darkness for at least one week to permit short-lived nuclides to decay. After being exposed to light of 552 nm for a period of time, the samples were then dissolved in solutions containing PO_4^{3-}, PO_3^{3-} and PO_2^{3-} carriers. Three aliquots were taken from the sample solution: from the first ^{32}P was determined as PO_4^{3-} ion, in the second aliquot ^{32}P was determined as PO_3^{3-} and PO_4^{3-} and in the third ^{32}P was determined as PO_2^{3-}, PO_3^{3-} and PO_4^{3-}. In all cases, the ions to be separated were converted to PO_4^{3-} and precipitated

as $NH_4MgPO_4 \cdot 6H_2O$. The activity in each precipitate was counted with a low-background methane-flow counter.

The percentage of ^{32}P activity in each oxidation state was determined as a function of photo-annealing time. Complex curves were obtained, indicating both oxidation and reduction occurring during annealing. A least squares statistical analysis of the results was done using a computer program to find the best fit of the points.

There is a marked difference among the three salts, not only in the distribution of ^{32}P activity among the three oxidation states, but also in the characteristics of the photo-annealing curves. The first suggest a cation effect (Li^+, Na^+ and K^+) and the second the effect of different impurities varying both in nature and quantity from one alkali chloride to the other.

An attempt was also made to study the hot atom chemistry of ^{32}P produced by $^{30}Si(t,p)^{32}Si \xrightarrow[700\ y]{\beta^-} {}^{32}P$ reaction in silicon dioxide and sodium silicates.

Lithium silicide alloy enriched with 90% ^6Li, 70% by weight of silicon was prepared and irradiated at various reactors to obtain ^{32}Si by the action of tritium atoms produced by $^6Li(n,\alpha)T$ reaction. After irradiation the samples were decomposed in closed systems with sodium hydroxide solution; SiO_2 produced this way was further used to prepare Na_2SiO_3 and Na_4SiO_4. The samples were stored at five different temperatures: -196°, -78°, 0°, 20-25° and 100°C. for at least a month for ^{32}P to accumulate. It was intended to analyze for $^{32}PO_4^{3-}$, $^{32}PO_3^{3-}$ and $^{32}PO_2^{3-}$ ions, but enough activity could not be obtained to make sensible comparisons. For each ion about 1-3 cpm were obtained on a low-background methane-flow proportional counter which has a background of 0.5-2.0 cpm.

This project was abandoned because of difficulties in obtaining sufficient ^{32}P radioactivity in the time available.

PART ONE

HOT ATOM CHEMISTRY OF ^{32}P IN ALKALI CHLORIDES

I. INTRODUCTION

A. Historical Background

Interest in the chemical effects of nuclear activation started as early as 1934. Szilard and Chalmers[1] studied the behavior of radioactive iodine atoms formed in neutron irradiated liquid ethyl iodide. They observed that most of the radioactive iodine could be extracted into water solution. The carbon-iodine bond had ruptured and had not reformed in a large percentage of recoil events.

Since that time studies of the chemical behavior of atoms activated by nuclear processes have provided information as to the secondary reactions of atoms which have freed themselves from their parent molecules as well as to the primary processes of bond rupture. As the subject developed, several types of nuclear activation in addition to the (n,γ) reaction, such as (γ,n), $(n,2n)$, (n,p), (n,α), (d,p) and (γ,p), were used.[2,3,4]

Originally the subject was studied as an investigation of the chemical consequences of nuclear events. More recently, however, it has been realized that nuclear activation is a useful and unique tool to examine certain kinds of reaction mechanisms. In the nuclear process a daughter atom is made not only radioactive, but is also energized. This property allows one to study "hot" atom reactions.[4] Even though hot reactions can be made to occur in various devices such as shock tubes and plasma torches[5] (where temperatures may reach 10,000°C) the entire system is completely altered (products as well as reactants), and the identification of fundamental processes becomes very complicated. In the method of nuclear activation, high

energy atoms are produced and these atoms can be directly identified in the reaction products.

The hot-atom chemistry of ^{32}P in alkali chlorides produced by ^{35}Cl (n,α) ^{32}P reaction has been studied by a number of people[6-14], but there is little agreement about either the initial valence distribution of the phosphorus or how this is affected by post-irradiation of the crystals. Aten[6,7] found in the 1940's that 70% of the total radioactive phosphorus in sodium chloride was in lower oxidation states. Caillat and Süe[8] found about 50% of radioactive phosphorus in lower oxidation states and also noted that this proportion was increased upon heating. Lindner[9] obtained results similar to Aten's. Carlsen and Koski[10] found that irradiation conditions had a pronounced effect upon the distribution of phosphorus valence states in potassium chloride. With a heavy reactor bombardment (10^{18} n/cm^2 total) lower oxidation states were only 4.7% of the total, while with 10^{14} n/cm^2 total, 64% and with 5×10^{10} n/cm^2, 82% were obtained in the lower oxidation states. This is in agreement with Aten who used a relatively low-dose source.

Butterworth and Campbell[11] investigated the oxidation states of ^{32}P species in potassium chloride lattices as a function of the gamma doses received by the crystal prior to and during neutron irradiation and as a function of thermal annealing at various temperatures. They found that gamma irradiation prior to neutron bombardment had a reducing effect on the ^{32}P recoils, although this effect tends to be destroyed at higher doses. They obtained thermal annealing curves with complex temperature dependence where both oxidative and reducing reactions occurred.

Later Cifka[13] studied the thermal- and photo-annealing of ^{32}P recoils in KCl. Unlike other investigators he maintained

his crystals at dry-ice temperature during irradiation and until analysis; and also, he was careful to exclude light at all times. The effects of thermal annealing are much larger in Cifka's work than in that of Butterworth and Campbell. He found that most of the dark thermal-annealing curves differed markedly from those obtained for the same neutron-irradiated crystals exposed to daylight during handling. The results of the photo-annealing with daylight and 552 nm light show that ^{32}P recoils are reduced, the rate of reduction being higher for P (III) recoils than for P (V) recoils. The percentage distribution of ^{32}P among its oxidation states in samples that were not subjected to either thermal- or photo-annealing was 65.6, 13.1 and 21.3 % for P (V), P (III) and P (I), respectively.

Recently Babtista, Newton and Robinson[14] published a paper on valence distribution of phosphorus in potassium chloride crystals. They used single crystals of potassium chloride obtained by the Stockbarger method after purification by zone-refining. In contrast to others they found most of ^{32}P in a hypophosphite, P (I), fraction on dissolution. The percentages were 24.0, 10.9 and 65.1 % for P (V), P (III) and P (I), respectively. Crystals containing OH ions or CO_2 and CO_3 impurity showed an increase in the phosphite, P (III), and phosphate, P (V), fractions at the expense of P (I). Introduction of defects either by crushing or quenching from a higher temperature, prior to irradiation, also increased the oxidized fractions.

Thus the distribution of the oxidation states of ^{32}P recoils depend upon many factors including purity and degree of imperfection, pre- and post-irradiation conditions.

B. Statement of the Problem

So far most of the work on ^{32}P produced by ^{35}Cl (n,α) ^{32}P reaction has been with potassium chloride. There has been no attempt to compare the valence distribution of ^{32}P in different alkali or other chlorides to study the effect of metal ion in a given period (size) and in different periods (oxidation state and crystal structure). It therefore seemed of interest to study the valence distribution and photo-annealing of ^{32}P recoils in some alkali chlorides, namely lithium, sodium, and potassium chloride and to compare the results of those obtained for potassium chloride.

II. GENERAL CONSIDERATIONS

A. Nuclear Reactions as a Source of Energetic Atoms[3,4,15]

As a result of a nuclear reaction or of radioactive decay from a higher to a lower nuclear level, the atom in which nuclear transofrmation has occurred may acquire kinetic, ionization and electron-excitation energies.

1. Recoil Kinetic Energy

An atom may possess kinetic energy as a result of three types of nuclear reactions: a) thermal particle induced-no particle emitted reactions, b) accelerated particle induced and/or particle emitted reactions, and c) spontaneous (decay) reactions.

a. Thermal Particle Induced Reactions

The most commonly employed reaction has been the (n,γ) reaction with thermal neutrons which have a kinetic energy of about 0.025 eV (that of any gaseous particle at 17°C). The kinetic energy is supplied to the radioactive atom not by the thermal neutron but by the binding energy ($\sim$ 5-10 Mev) released as a result of its capture by the nucleus. In the case of the (n,γ) reaction most of this binding energy is released in the form of electromagnetic radiation (gamma rays). A γ ray of energy E_γ has a momentum $p_\gamma = E_\gamma/c$. To conserve momentum the recoil atom must have an identical momentum and, therefore, the recoil energy $E_R = p_\gamma^2/2M = E_\gamma^2/2Mc^2$, where M is the mass of the atom. For M in atomic mass units and E_γ in Mev., we have[15]

$$E_R = \frac{537\ E_\gamma^2}{M}\ \text{eV}.$$

Recoil energies from (n,γ) processes have values of ~200-1500 eV.

Usually the energy is released not in a single quantum but in a cascade. This tends to lower the recoil energy in a fraction of nuclear transformations because of the possibility of partial cancellation of the momentum in different directions. The excited atom, as a result, may fail to rupture its bonds. To calculate the recoil energy spectra it is necessary to know the details of the deexcitation of the compound nucleus by multi-gamma quantum emission. However, the number of published recoil energy spectra has been limited to three[16-18] due to lack of sufficient details about the neutron capture γ-rays. Calculations based on the recently published capture γ-spectra[19,20] from the ^{50}Cr (n,γ)^{51}Cr process show that more than 98% of the recoil atoms will have a recoil energy larger than 50 eV. This is in agreement with ^{33}S, ^{36}Cl and ^{32}P systems.[16-18] However, all these are light nuclei. With heavier nuclei, the recoil energy spectrum may shift to lower values.

b. Induced Particle-Emission Reactions

When the nucleus is struck by a fast neutron or charged particle, part of the energy of the incident particle will be transferred as kinetic energy to the struck nucleus. Typical of such transformations are (n,2n), (n,p), and (n,α) reactions. In this case it is possible to achieve recoil kinetic energies in the range of 10^3-10^6 eV. For cases in which a single particle is emitted, Libby[2] has derived expressions for the average recoil energy $\bar{E}_m$ and the spread 2A.

$$E_M = \bar{E}_M - A \cos \theta$$

$$E_M = \frac{E\mu\ M\mu}{(M+m)^2} + \frac{E\mu\ m(m+M-\mu)}{(m+M)^2}\left(1 + \frac{Q}{E\mu}\left[\frac{m+M}{m+M-\mu}\right]\right)$$

$$2A = \frac{4E\mu}{(M+m)^2}\sqrt{Mm\mu\,(m+M-\mu)\left(1 + \frac{Q}{E\mu}\left[\frac{m+M}{m+M-\mu}\right]\right)}$$

where μ = mass of incident particle, M = mass of recoil atom, m = mass of emitted particle, E_M = energy of recoil atom, E_μ = energy of incident particle in MeV and Q = internal energy released.

Complication arise in the case of two particle emission such as the (n,2n) reaction, since the angular correlations of the particles must be considered. In any case high energy bombardment and/or particle emission results in kinetic energies several orders of magnitude greater than thermal neutron capture.

c. Decay Processes

Atoms also receive kinetic energy upon emission of particles during radioactive decay from a higher to a lower nuclear energy level. In the case of alpha decay, to conserve momentum, the radioactive atom acquires kinetic energy, $E_M = \frac{m}{M} E_\alpha$, where m is the mass of α particle, M is the mass of the radioactive atom and E_α the energy of the alpha particles. In beta and positron decay processes the recoil energies cover a spectrum due to the variable partition of momentum between β particles and neutrinos. The case of recoil from beta emission has been treated by Libby[2] assuming no angular correlation between beta particle and neutrino. Edwards and Davies[3] have discussed the case in which such

correlation exists. Assuming different β-neutrino interactions the energy spectrum of recoils from β-emission by ^{14}C has been calculated.[21] A great proportion of the recoil atoms have an energy less than 10-15 eV.

2. Ionization Energy

Ionization may result from several processes, one of which is internal conversion of gamma quanta in isomeric transitions or (n,γ) reactions. An Auger or vacancy cascade can result upon loss of a K or L shell electron, giving a charge of several units at the periphery of the atom. Electron capture by the nucleus leading to a vacancy in an inner shell can also initiate an Auger process. Measurements of the charge acquired by halogen atoms as a result of (n,γ) reactions and isomeric transitions have been made by Wexler, Davies and collaborators.[22-25] Later charge spectrometry was developed to investigate the relative probabilities of loss of one, two, three, or more electrons following the nuclear event.[26] It is found by charge spectrometry that the Auger cascade leads to a more or less symmetrical distribution of charge from +1 to +15 with a maximum at about +8.

When a nuclear transformation such that a change in charge, $\Delta Z \neq 0$, occurs, there is a change in the nuclear field strength causing expansion of the extranuclear shells when $\Delta Z < 0$ and contraction when $\Delta Z > 0$. If the rearrangement of the electron shells is slow relative to the nuclear process, considerable electronic excitation can occur and ionization may result. Ionization from this cause has been termed "shake-off".[27] Charge spectrograms have been obtained for β^- or β^+ emission processes.[26-29] There is usually no electron loss, so that charge of +1 or -1 dominates in the spectrum, followed by a distribution resulting from loss of outer electrons,

dropping off sharply towards higher charge values. Comparison of the charge spectra shows that isomeric transition with an Auger cascade should have violent chemical effects for the molecule in which it occurs, whereas the effects of "shake-off" should be milder.

Interaction of a charged particle such as β^-, p, d or α emitted from the nucleus directly with an extranuclear electron causes the ejection of the electron, resulting in ionization. The probability of direct ejection of an electron by a β^- particle is two or three orders of magnitude less than the probability of ionization by "shake-off".[30,31] Ejection of an electron in alpha particle emission is more probable than in beta emission. The charge on atoms of RaD recoiling after alpha emission by RaC has been measured and found to be +2 and a similar charge is found in the decay $Rn \rightarrow Ra\ A + \alpha$.[32,33]

If an atom recoils with an energy such that its velocity is greater than that of a peripheral electron, that electron will be lost. This form of ionization is called autoionization. The energy of the recoil should be greater than $10^3 \times M$, where M is the mass of the recoiling atom in a.m.u., for autoionization to occur. Thus this type of ionization is important only in heavy particle emission, fission, and nuclear reactions with fast incident particles. In the case of ^{235}U fission, the lighter fragment has a recoil velocity of $\sim 1.5 \times 10^9$ cm/sec and will lose $\sim$10-20 electrons by autoionization.[3]

3. Electronic Excitation Energy

Electronic excitation may occur in those processes in which a change of nuclear charge takes place more rapidly than the readjustment of the electron shells. The energy of

excitation is given approximately by the following equation for the case of nonadiabatic emission average[34]:

$$E_{exc} = 24.47\ Z^{1/3}\ (Z' - Z)^2\ \text{eV}.$$

where Z and Z' are the nuclear charges before and after emission. For a ^{14}C atom beta particle emission thus imparts an energy of 59 eV to the electron shells.

Electronic excitation may also occur as a result of neutralization of the charge acquired by nuclear transformation. Magee and Gurnee[35] have done calculations for the reaction,

$$HBr^{4+} + HBr \rightarrow HBr^{3+} + HBr^{+}$$

and estimated that as much as 30-40 eV may be available for excitation of the electrons of the products. Such excitation occurs due to crossover of the potential energy curves for an ion-molecule pair with curves for excited states of one member of the ion pair which results from charge transfer.

Thus in a single nuclear process there is a possibility of obtaining more than one mode of activation. A marked atom of an (n,γ) reaction will have recoil energy but may also acquire charge by internal conversion of some of the softer quanta in the gamma cascade. Neutralization of this charge during recoil may cause excitation of the extranuclear electrons.

B. Chemical Behavior of Energetic Atoms

An atom in which nuclear transformation has occurred possesses sufficient energy in the form of kinetic, ionization or electronic excitation to rupture its bonds. Calculations by Wiles and Wong[36] show a high probability of the transformed

atom's escape even from compounds in which it is almost completely enclosed. Under conditions such that the possibility of recombination is unlikely, observed retention is low.[4] This indicates that in most cases initial bond rupture occurs. The hot atom or ion once freed from its chemical bonds dissipates most of its excess energy along its recoil path and loses its charge through successive interactions. Near the end of its recoil path with about 10 eV energy, it reacts with its environment. In this energy region unusual "hot" reactions occur. If a hot atom escapes this energy region without reacting and falls to the thermal energy region (0.025 eV) it may undergo a more familiar activation-energy-controlled chemical reaction.

Several models have been developed to explain the observed behavior of hot atoms in the gas, liquid, and solid states. The models pertaining to gases and liquids will be sketched only briefly since this thesis is concerned with hot atoms in solids.

1. Gases

In 1960 Estrup and Wolfgang[37] developed a kinetic theory of hot atom reactions in the gas phase. These reactions differ from energy interactions in that $E \gg \Delta E$, so that $\exp(-\Delta E/RT) \approx 1$ in the equation $k = pZ \exp(-\Delta E/RT)$. The Estrup-Wolfgang theory assumes that a) the recoil atom loses its energy in inelastic collisions; b) the recoil has a high initial energy, E_o, and that when the energy has been reduced by collisions into a range, E_2-E_1, retention-causing reactions can occur; c) E_o-E_2 is sufficiently large for a number of collisions to have been made before the E_2-E_1 range is reached, so that a statistically well defined distribution of energies prevails within this range; d) $E_1 \gg$ thermal energies.

Estrup and Wolfgang[38] investigated the $^{3}He(n,p)^{3}H$ reaction in CH_4 with inert gas moderator. $H^{3}H$, $CH_3{}^{3}H$ and $-CH_2H_3$ were proposed to be formed by hot reactions. Small amounts of ion scavengers such as I_2 gas did not affect the yield of these products. There was a marked depression of the $H^{3}H$ yield due to thermal abstraction of H from CH_4 or of the combination of thermalized ^{3}H with radiation-formed species to from higher tritiated hydrocarbon. The presence of excess helium reduced the yield of the hot products by acting as moderator. Altering the temperature during the irradiation did not affect the yield of hot products. All these point out that the reaction was a "hot" one.

The Wolfgang-Estrup theory assumes energy loss by elastic collisions. This assumption is valid for monatomic inert gas moderators in methane but not necessarily applicable in other cases. Later Gordus[17,39] announced a hot atom reaction model based on the treatment developed by Miller et al.[40,41] This model accounts for some data that could not be explained by Wolfgang-Estrup theory.

2. Liquids

Several models have been proposed to explain the behavior of hot atoms in the liquid phase. Some of the earlier models were extended and modified. Libby's[2] elastic collision "billiard-ball" model assumes head-on elastic collisions of hot atoms with other similar mass atoms. Most of the energy can be transferred to the struck atom which may be dislodged from its chemical bonds. If the recoil atom is left with kinetic energy below a certain critical value necessary for escape from the collision site, bond formation will occur between the recoil and the molecular residue, leading to higher retention values. Otherwise, with kinetic

energies exceeding $\sim$20 eV, the hot atom possesses an energy greater than bond energies and the effective duration of the collision is very much less than the time required for intramolecular vibrational relaxation; the energy is inefficiently transferred along the bonds.

Epithermal reaction schemes[42] were proposed as modifications to the billiard-ball model. This reaction mechanism focuses attention on the epithermal energy range of a few eV in which the recoil can form an excited complex with an organic molecule which decomposes into various products containing the radioactive atom. Both of the models involve "hot" highly localized reactions.

Elastic-collision models could not account for all high-energy organic retention in the liquid phase. Soon there was evidence for the occurrence of inelastic collisions during recoils in liquids leading to fragmentation of molecules and that the radioactive atom combining with these fragments. These findings were the basis of the random fragmentation model of Willard.[43]

Later Milman[44] modified the kinetic theory of Wolfgang and Estrup and applied it to liquid systems. The investigation was limited to reactions of bromine in highly hydrogenated or highly halogenated media. The principal aim was to obtain from experimental data an indication of the mechanism of collisional energy degradation.

To explain the observed temperature effects for hot reactions Shaw[45] has developed a physico-chemical model in which he considers the behavior of the liquid in the immediate vicinity of the neutron capture event. The model ignores the possibility of charged particles. Shaw also proposed another model in which the liquid is considered as a melted solid.[46]

3. Solids

a. Hot Zone Model

The Hot Zone Model was proposed by Harbottle and Sutin in 1958.[47] It is based on the Seitz and Koehler[48] treatment of the slowing-down of energetic particles and makes use of the "displacement spike" concept put forward by solid state physicists.

As a result of nuclear activation a free radioactive atom in a state of high energy is formed. During the slowing down of this recoil atom two energy regions are distinguished:

a) the hot region: all reactions occurring before the recoil atom reaches thermal equilibrium with its environment fall in this energy range ($E > \sim 0.025$ eV);

b) the thermal region: in this energy range ($E \sim 0.025$ eV) the radioactive atom is able to diffuse through the surrounding medium and undergo familiar chemical reactions such as addition, substitution, recombination, exchange, etc. These are the annealing reactions.

In the hot region the reactions are of two general types: a) those proceeding by the direct replacement of an atom in a molecule by the recoiling atom in a collision, b) chemical reactions such as occur in the thermal region but modified by the higher local temperatures.

First the recoil atom is assumed to be neutral and moving relatively slowly and to lose its energy entirely by elastic collisions. There are two types of elastic collisions: Rutherford scattering and hard-sphere scattering depending on the degree of screening of nuclear coulomb interaction. The coulomb field of the nucleus of the atom is screened by the orbital electrons so the scattering

deviates from the pure Rutherford law. It was assumed[47] that the screened interaction potential between two identical atoms of atomic number Z, at a distance r is given by

$$V = \frac{Z^2e^2}{r} e^{-r/a} \tag{1}$$

where a is a screening constant having the form

$$a = \frac{\lambda a_h}{Z^{1/3}} \tag{2}$$

where λ is a constant and is equal to 1 and a_h is the Bohr radius of the hydrogen atom. For moderately heavy atoms a is approximately equal to the radius of the atomic electron cloud.

The parameter L = b/a defines the regions of Rutherford and hard-sphere scattering (b is the distance of closest approach). For $L>1$, the nuclei of the two colliding atoms will not penetrate substantially each others' electronic shells. This is the condition for hard-sphere scattering. If $L<1$, appreciable interpenetration of the electron shells will occur, known as Rutherford scattering.

For ionic crystals, E_d (the energy required to displace an atom to an interstitial position) is $\sim$25 eV. The total number of displacements, primary as well as secondary, can be calculated as a function of recoil energy. Phosphorus-32 from the $^{35}Cl(n,\alpha)^{32}P$ reaction will have an energy of about 0.50 Mev. To calculate the number of displacements, one uses the formula[48] $g(X_1) = 0.561(1 + X_1)$ where $X_1 = E/E_d$ to obtain 1.12×10^4 displacements. In molecular crystals an atom of 300 eV energy will produce about 17 displaced atoms. In a complex crystal such as $KMnO_4$ there will be more displaced atoms than the above calculated value because of the less

efficient collisions where a recoil atom strikes an atom of different mass.

In complex crystals there is the possibility of energy loss by inelastic collisions by two processes. When the recoil atom is moving slowly ($E \sim 10$ eV) enough time is available for its coulomb field to interact with that of a whole molecule which may then dissociate as a result of vibrational excitation. This can occur during the life time of the hot zone. The second process involves a direct collision of the recoil atom with a bound atom such that the struck atom becomes vibrationally excited and bond rupture results.

Replacement processes are also important in the hot zone. A moving atom with energy less than E_d may still have enough energy to replace an atom and push it into an interstitial position. The expression for the number of replacement collisions, N_ρ, occurring as a function of N_d, the number of displacement collisions, and of E_ρ and E_d is

$$N_\rho = 0.5\ N_d \left[1 + \log \left(\frac{E_d}{E_\rho}\right) \Big/ \log\ (4/3)\right] \qquad (3)$$

For KCl, $E_\rho \approx 8$ eV, $E_d = 25$ eV and $E = 0.50$ Mev,
$N_\rho = 2.8 \times 10^4$

$$\frac{N_\rho}{N_d} = 2.5$$

A high energy atom displaced from its position in the solid lattice causes other atoms to be displaced. All the displaced atoms will dissipate some of their energy by exciting lattice vibrations corresponding to a high temperature. The solid will thus contain a localized volume, called a hot-zone. The size and the duration of the hot-zone can be calculated.

If hard-sphere collisions are assumed near the end of the recoil path, the mean free path can be calculated. The collision diameter can be taken as the interatomic distance at which the screened interaction potential, V, is equal to the kinetic energy of the moving atoms. Rearranging equation (1) we get the approximate radius, R, for hard-sphere collisions between identical atoms

$$R = a \ln \frac{Z^2 e^2}{R E} = \frac{\lambda a_h}{Z^{1/3}} \ln \frac{Z^2 e^2}{R E} \quad . \tag{4}$$

As E decreases, R increases and $E \to E_d$, $R \to$ atomic radius, r_s, defined by

$$\frac{4}{3} \pi r_s^3 = \frac{1}{n_o} \tag{5}$$

where n_o is the number of atoms per cc. The mean free path is the reciprocal of the cross section of a collision atom times the number of atoms per cc.

$$L_s = \frac{1}{\pi R^2 n_o} = \frac{4}{3} \frac{r_s^3}{R^2} \tag{6}$$

For an atom of energy 300 eV the mean free path $L_s = 5\ r_s$. Thus it is of the order of atomic diameters.

A recoil atom of energy 300 eV of mass 100 and $L_s = 5\ r_s$ will have a velocity of 2.4×10^{14} Å/sec. Four collisions are necessary to reduce the energy below 25 eV. The total time required for this process is $4L_s/v_i = 1.3 \times 10^{-13}$ sec. Thus nearly all the energy is deposited in a sphere of radius $5\ r_s$ in about 10^{-13} sec. This will produce a very high local temperature. The individual collision hot

spots merge to form a displacement spike or hot zone within 10^{-13} sec.

In the hot zone a recoil atom has a good chance of undergoing some chemical processes such as free radical recombination, charge transfer, ion-molecule reactions, exchange reactions and diffusion jumps. However, if the reactants are not nearest neighbors, they will have to diffuse to encounter each other, which takes time. Steric factors are also important and might slow the reaction when complex ions and molecules are involved. So instead of the usual equation for the frequency of a process:

$$v = v_o e^{-F/kT}$$

where F is the energy of activation,

$$v = (KT/h)\, e^{\Delta S^{\neq}/k}\, e^{-\Delta H^{\neq}/kT} \qquad (7)$$

is used by Harbottle and Sutin. $\Delta S^{\neq}$ term takes steric and other probability factors into account.

b. Disorder Model

In 1965 Müller[49] proposed the disorder model to account for the chemical consequences of the $^{185}Re(n,\gamma)^{186}Re$ reaction in mixed crystals of $K_2ReBr_6 - K_2SnCl_6$. Later Cairns[50] supported the model with experiments done on neutron irradiated single crystals of potassium iodide.

Müller investigated the $^{185}Re(n,\gamma)^{186}Re$ reaction for $K_2ReBr_6 - K_2SnCl_6$ in the range from 1 to 28 mol-% K_2ReBr_6. He obtained all the $ReCl_nBr_{6-n}^{2-}$ species, where n = 0, 1, 2,...,6. According to the hot-zone model a statistical distribution of these species should be expected. Calculated

values of $[ReCl_nBr^{2-}_{6-n}]$ according to equation (8), where the concentration of each species is expressed as a function of Cl and Br concentrations, did not agree with the experimentally obtained values.

$$[ReCl_nBr^{2-}_{n-6}] = \binom{6}{n}[Cl]^n[Br]^{6-n} \quad n = 0,1,2,....,6 \qquad (8)$$

Recoil atoms leave their normal lattice sites and escape into the lattice, lose their kinetic energy rapidly, and finally come to rest. In the case of an (n,γ) process, the resting place is in the immediate vicinity of the starting point, that is, a few lattice points away. The recoil atoms generate around their starting point only small changes in the lattice arrangement without producing a melt so the fate of the recoil atom is determined by the structure of the immediate environment it has reached after having lost its kinetic energy. The recoil atom at rest may be in the form of a chemical compound or it may be in a metastable state, disorder center, which can be annealed.

c. Depleted Zone Model

The basic event in an irradiated solid is the production of an energetic primary atom by a collision with an incoming particle such as neutrons, deuterons, etc. During the slowing-down process the primary atom can travel over a certain distance, the "range", the linear dimension of the zone where the primary can produce physical changes. Usually the ranges are calculated in a randomized way which does not take into account the crystal structure which my be highly anisotropic.

Silsbee[51] was the first to emphasize the importance of focusing effects in radiation damage experiments on account of the regularity of crystals. He illustrated this possibility

by considering the transport of energy (not of matter) along a linear chain of atoms interacting with each other like hard spheres. The transfer of energy in low index crystallographic directions is called focusing and the interaction of atoms a focusing collision or focuson. In addition to focusons, dynamic crowdions are also produced. They differ from focusons in that they transport not only energy and momentum, but also both energy and matter. In a focusing collision all the atoms are left in their original sites except the last one which moves away. In a dynamic crowdion propagation, each atom in the collision chain moves into the position of its nearest neighbor and the vacancy is at the origin rather than at the end of the collision chain. Lehmann and Leibfried[52] investigated the effects of long-range channeling. They found, in agreement with the machine calculations of Robinson, Holmes, and Oen[53,54] that a primary atom or ion moving along channels bordered by close-packed atomic chains or planes, experiences relatively small interaction; the rate of energy loss is low and the range is thus greatly increased.

The long range transport of atoms and energy leads to a specific kind of defect, the depleted or diluted zone proposed by Seeger.[55] At the zone a high local density of vacant sites are formed, which are surrounded by a few nearby interstitials and a substantial number of distant interstitials that were separated from the vacancies by the Crowdion mechanism. A depleted zone has a maximum diameter of about 20 Å around a recoil atom.

Cairns and Thomson[50] later supplied experimental evidence for this model. They showed that iodine atoms were ejected from thermal-neutron irradiated single crystals of KI in certain preferred directions.

d. Defect Model

Maddock[56,57] has emphasized the role of defects present in the crystal lattice in effecting chemical changes in the state of recoil atoms. In a study of neutron-irradiated potassium chromate he observed that the retention and the annealing characteristics following neutron-irradiation were dependent to some extent on the treatment of the crystal before irradiation. Pre-irradiation treatments such as crushing, quenching from a high temperature, subjection to ionizing radiation, and doping with multi-charged cationic impurity all sensitize the neutron-irradiated material to subsequent thermal annealing. The effect of each one except doping is eliminated by thermal annealing prior to irradiation. Anion-doped crystals showed increased resistance to thermal annealing.[58] Post-irradiation thermal and radiation annealing increase the initial retention, but when both are used together, the final retention depends upon the order of their administration.

Maddock explained all these and other[59,60,61] experimental observations by a defect model. He postulated that the thermal annealing event requires the participation of some defect, in the case of potassium chromate a vacancy. Defects diffuse towards the fragments when close to them. Initially the defects are uniformly distributed throughout the crystallites at a much greater concentration than the ^{51}Cr fragments. During the fast stage of annealing those fragments separated from defects by less than some critical distance combine rapidly, the process being first order with respect to the fragments. The fragments and defects behave as associated pairs. The critical separation radius increases with the annealing temperature. During the slow-annealing stage there is a slow diffusion of defects,

initially separated from the fragments by a larger-than-critical distance, into the reacting regions. The rate of diffusion is constant since the total supply of defects is large compared to the number of fragments, so the annealing proceeds as a zero-order process.

The cation-doped crystals showed unusual insensitivity toward radiation annealing. This was explained by Maddock in the following way: the presence of vacancies introduced in the crystal by means of multicharged impurity cations which provide centers that compete with the fragments for the electrons or excitons. A high vacancy density in alkali halides facilitates the formation of F centers by trapping electrons.[62] Vacancies also serve to dissipate the exciton energy. Hence the doped crystals are rendered insensitive to radiation annealing.

Anion doping by phosphate somewhat increased the resistance of the chromate to thermal annealing although the effect is much smaller than the cation doping. Cation vacancies facilitate the formation of V centers during the irradiation. These defects act as electron traps, facilitate the oxidation step in thermal annealing. The anion vacancies, on the other hand, behave as F centers and compete with the radioactive fragments for the available electron traps during thermal annealing. Thus the anion vacancies make thermal annealing more difficult.

e. Variable Depth Electron Donor Model

The variable depth electron donor model was proposed by Shankar, Nath and Thomas.[63] It is an extension of Maddock's theory of thermal annealing. The model postulates the formation of electron traps of variable depth in the bulk of the irradiated material. There are three types of electron donors or traps. One of them is due to pre-existing

crystal defects, another to extraneous radiation (gamma radiation and fast neutrons), and the third is produced in the recoil track as a result of fragmentation and Auger processes. During post-irradiation thermal annealing, electrons are emptied out from these traps with characteristic half-times depending on their depth and the released electrons take part in the annealing.

This model received support from Rao and Nath[64] who observed that the rate is enhanced when annealing in some cobalt complexes is carried out in electron donating ambients of acetone or alcohol vapors. This model was further supported by Andersen and Olesen[65] from their experimental results based on thermoluminescence and conductivity "glow curves" of neutron irradiated K_2CrO_4.

None of these models considered here is able to interpret all of the existing data. Experimentation aided by computer simulation[66] of three dimensional atomic motions might provide a more general model.

C. Annealing Reactions

The regeneration of the original physical and chemical properties of irradiated solids is called annealing. Annealing reactions, however, also refer to post radiolytic and recoil reactions in irradiated solids, although a reversion to the original physical or chemical properties is not obtained by the post irradiation treatment. There are four types of post radiolytic treatments: thermal, radiation, light, and pressure.

The annealing behavior of irradiated solids is complicated and not yet well understood in spite of the availability of a large amount of data both in simple and complex systems.

1. Thermal Annealing

Thermal annealing reactions differ from system to system depending on the physical and chemical properties of the host crystal. The stability of the radiolytic species varies widely with the crystal matrix. The concentration and kind of defects in the crystal introduced by grinding, irradiation or by doping with foreign cations have a strong effect on the subsequent course of the thermal annealing reactions. Another factor is the nature of the nuclear transformations which lead to the recoil atom.[67]

A typical isothermal annealing curve is shown in Figure 1.[68] The yield of a particular recoverable labelled species (usually the parent molecule) is plotted against time. It shows an initial rapid change followed by a plateau in which change is very slight. At a higher temperature the curve rises rapidly, the plateau is reached at about the same time but at a higher level.

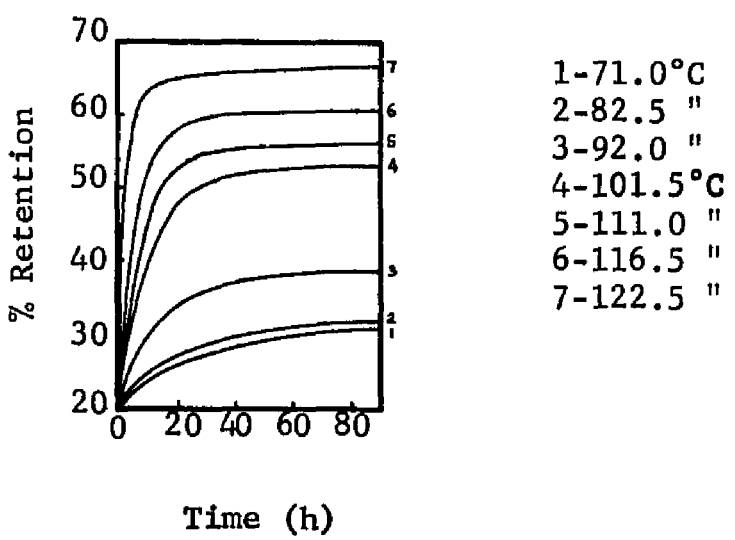

Figure 1

Isothermal Annealing of ^{60}Co Recoil Atoms

If neutron irradiated crystals are annealed isothermally up to the plateau and then the temperature is increased a new phase of the rapid growth takes place with a new plateau characteristic of the higher temperature. Unlike ordinary reactions in solution, the annealing reactions do not seem to go to completion at a given temperature, but rather to go more slowly as time proceeds.

The yield or retention increase from the beginning of the annealing curve to the plateau can be described by a simple empirical rule. The increase (ΔR) is proportional to the inverse of the absolute temperature, Figure 2.[69]

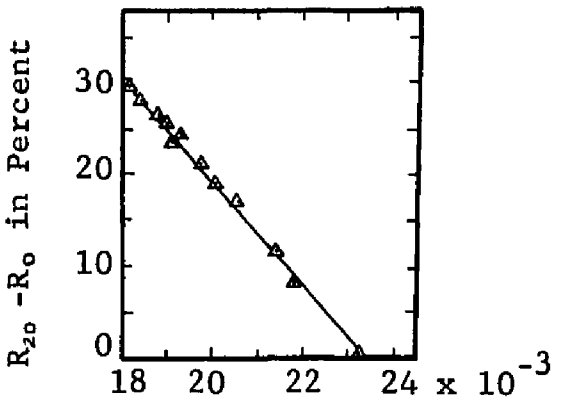

Figure 2

"Maddock's Rule"

It is postulated by Maddock and co-workers[56-60] that the thermal annealing event requires the participation of some defect such as a vacancy, and that the defects diffuse preferentially towards the fragments when close to them. A recoil atom may come to rest in an interstitial position. A vacancy can be considered as a trap consisting of any fragment or species capable of reacting chemically with the

interstitial atom. Maddock's proposed mechanism is discussed at some length in the Defect Model section.

Later it is proposed[70,71] that during thermal annealing all types of defects are liberated. The liberated charge carriers may undergo annihilation or be trapped by some other crystal defects at the recoil atoms or at the regions surrounding the recoil atoms. Thus trapped charge carriers are responsible for the observed chemical changes. Experiments on potassium chromate doped with thallium ions indicated a more complex thermal annealing mechanism than assumed by Maddock's model. A mechanism involving a combination of reduction and oxidation processes is considered to be more probable. Butterworth and Campbell[71] studied ^{32}P recoils in neutron irradiated potassium chloride and obtained evidence for a thermal annealing mechanism involving cycles of reduction and oxidation processes.

2. Photo-annealing

Bleaching of radiation induced centers by ultraviolet light has been known for more than forty years.[72] The optical bleaching processes have been studied in alkali halides and have yielded important information about radiolytic defects. Annealing of recoil damage by ultraviolet light was first reported for neutron irradiated potassium chlororhenite by Herr[73] in 1952, but no photo-annealing effect was observed for the chromate system. This might be due to a high absorption coefficient of incident radiation, thus limiting the effect to a superficial layer of the crystal. Since then there has been a large number of photo-annealing experiments in various systems.[74-76]

There is a strong evidence that the chemical changes observed in nuclear recoil atoms during thermal annealing of

chromates is a result of activated charge carriers, electrons or holes.[56,57] Thus a close relationship exists between changes in the chemical valence states of the nuclear recoil atoms and the bleaching of the color centers formed during the neutron irradiation.

In 1950 Sūe and Caillat[8,77] reported that the distribution of the ^{32}P recoil atoms between different valence states obtained on dissolution of the irradiated potassium chloride was influenced by bleaching of the color centers before dissolution. Butterworth and Campbell[71] suggested a relation between the recoil ^{32}P atoms and the F-centers to explain the annealing phenomena in neutron irradiated potassium chloride. Positive holes might be responsible for the oxidative processes and F-electrons for the reducing processes.[78,79]

Cifka[13] carried out experiments on the photo-annealing of ^{32}P recoils in potassium chloride. He used 552 nm light for photo-annealing. The results are shown in Figure 3.

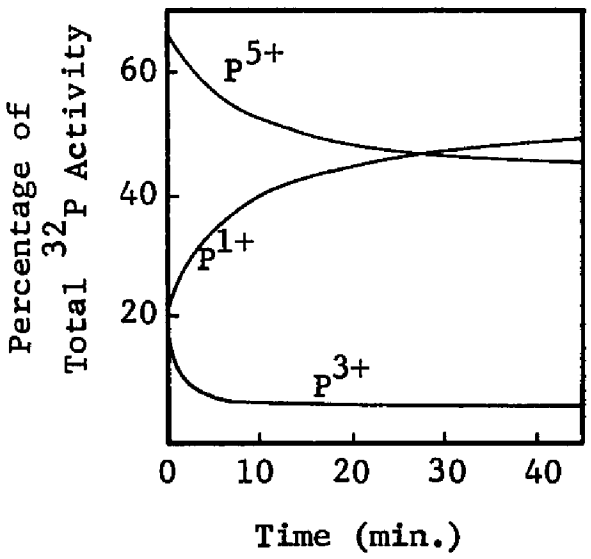

Figure 3

Photo-annealing of ^{32}P Recoils with 552nm Light

The ^{32}P recoils are reduced by the light, the rate of reduction being higher for P^{3+} recoils than for P^{5+} ones. The reduction of ^{32}P recoils can be explained by the existence of color centers in alkali halides as the relatively stable products of radiation damage of these materials. The optical spectra during the bleaching with 552 nm light also show a similar trend, that is, the concentration of F-centers decreases with time of annealing (Figure 4).

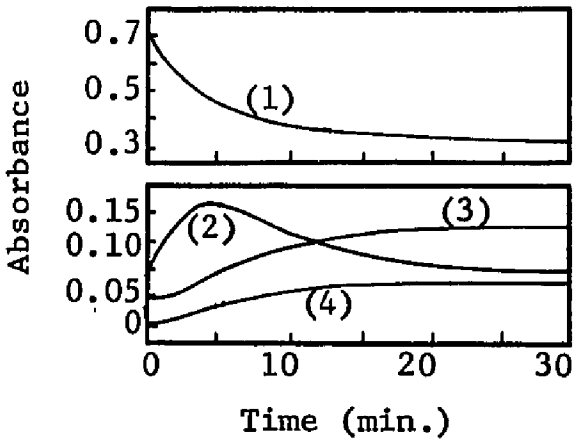

Figure 4

Change of absorbance for various centers during the bleaching with 552 nm light.[80] (1) F center; (2) M center; (3) R_2 center; (4) R_1 center.

The following processes are suggested by Cifka to occur during the illumination:

a) the excitation of the F-centers with the incident light

$$F + h\nu \rightarrow e^- + \alpha \qquad (9)$$

where $h\nu$ is a photon absorbed in the F band and α is a negative ion vacancy;

b) the reaction of free electrons, e^-

$$e^- + \text{hole} \rightarrow Cl^- \quad (10)$$

$$e^- + F \rightarrow F' \quad (11)$$

$$e^- + \alpha \rightarrow F \quad (12)$$

$$e^- + {}^{32}P^{+n} \rightarrow {}^{32}P^{+(n-1)}, \text{ etc.} \quad (13)$$

where F' denoted an F center that has trapped an electron and $^{32}P^{+n}$ denotes the ^{32}P recoils:

c) the secondary reactions

$$F' \rightarrow F + e^- \quad (14)$$

$$F' + F \rightarrow M + e^- \quad (15)$$

$$F' + \alpha \rightarrow M, \text{ etc.} \quad (16).$$

The reactions which lead to R_1, R_2 or other centers must also be taken into consideration. However, the most important reaction is (9) because the concentrations of other centers are very small compared to F centers. Reaction (13) accounts for the decrease of oxidation number of ^{32}P recoils.

The rate of reduction thus depends on the F center concentration, but it is a more complex reaction and depends also on the electron affinity of the given ^{32}P recoil or the complex formed by ^{32}P recoil and the crystal lattice (including imperfections). The intermediate P^{3+} has a rate of reduction approximately the same as the decrease of the F centers. Thus the reaction of the P^{5+} recoils can be considered as the rate-determining step for all four consecutive reactions with electrons yielding in the P^{1+} complex.

3. Radiation Annealing[15]

Radiation annealing of recoil atoms was first reported to occur during reactor irradiation in 1948.[80] Subsequent investigations[12,61,56,59,74,71,81] have shown that radiation annealing can be initiated by α particles, electrons, γ-rays and x-rays. The radiation recoil annealing reactions can be accounted for by three types of reaction: a) oxidation processes, b) formation of dimeric and polymeric recoil fragments, and c) processes involving rearrangement of the ligand distribution in complex metal ion systems.

The radiation annealing processes are influenced greatly by the presence of crystal defects. Doping potassium chromate with foreign ions, Ca^{2+}, represses the radiation annealing processes.[56] Thermal annealing before radiation annealing and heating during irradiation lead to an enhanced radiation annealing rate.

During the initial part of the radiation recoil annealing process, first order kinetics accurately describe the data. At higher doses, above $\sim$75 Mrads for potassium chromate, a deviation from first order kinetics is observed.[12,81,82] At very high doses radiation recoil annealing no longer takes place. There are three possible mechanisms for radiation recoil annealing: a) a thermal mechanism, the process taking place in or near the thermal spikes produced during degradation of the ionizing radiation of the crystals, b) a radical mechanism involving recombination of the recoil atom with ions or radicals produced by radiation, and c) a mechanism involving reactions dependent on the crystal defects present or generated in the crystals. Maddock has shown that only the last mechanism can account for all the available experimental data.

4. Annealing by Compression

Annealing by compression of nuclear recoil products was first reported for potassium chromate.[83] Compression of neutron irradiated crystals produced two effects[84]: the first, a rapid increase in the yield of the radioactively labelled target molecule (the retention), directly induced by the application of pressure, and the second, an acceleration of the thermal annealing processes. The first effect has been observed in all systems investigated, whereas the second effect was not observed in potassium dihydrogen arsenate.[85] A plastic flow process might be involved in the rapid annealing. Plastic deformation under stress leads to the movement of dislocations which in turn can increase their number and create new point defects.[86] The heat generated by slipping of the dislocations can produce ionization of electronic defects. The liberated charge carriers can interact with each other or be trapped at crystal defects, and so take part in the annealing processes. The large concentration of crystal defects introduced during compression may cause a decrease in the energy of activation for the subsequent thermal annealing reactions. The relationship between annealing by compression and thermal annealing was further investigated in irradiated potassium bromate.[87] The retention is increased after compression. This can be accounted for by the annealing of the radiolytic fragments in the crystal.

D. Alkali Chlorides

1. General Properties[86]

All alkali halides have a simple but highly symmetrical atomic arrangement, the unit cell of which is a cube. The three chlorides studied in this work have face-centered cubic lattices. The atomic arrangement in the face-centered cubic

lattice of lithium, sodium, and potassium chloride is shown in Figure 5.

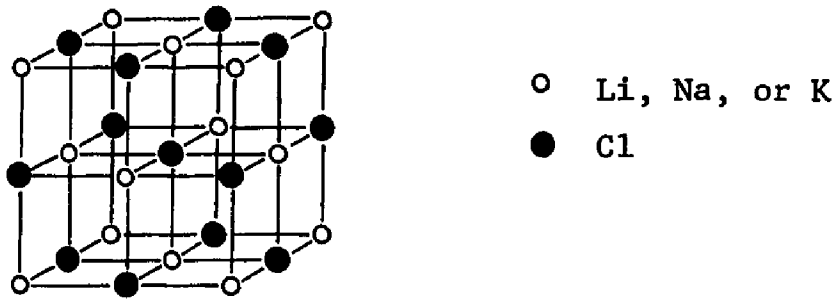

Figure 5. The Face-centered Cubic Lattice

In this structure each cation (alkali metal ion) is surrounded by six nearest-neighbor anions (chloride ions) and each anion by six nearest-neighbor cations. If we take the corner of the unit cell to be the center of a cation, there are also cations at the center of each face, the lattice being a face-centered one.

The alkali chlorides are typical ionic compounds. At normal temperatures they are highly insulating solids. As the temperature is raised, the electrical conductivity increases very rapidly, the carriers of electric charge being ionic in nature rather than electronic. They show optical transparency from the far ultraviolet to the far infrared.[88] There is thus a very broad spectral region in which changes in optical absorption can easily be detected and studied. Many chemical impurities when incorporated in the alkali halide crystals even in parts-per-million concentration introduce absorption bands in the normally-transparent spectral region. Defects and centers arising from other causes such as

mechanical deformation or ionizing-radiation also give rise to new absorption bands in this region.

2. Imperfections

a. Inherent Imperfections[86]

Crystalline solids are characterized by a regular and highly ordered structure. The unit cell repeats itself regularly in the lattice. This internal regularity is suggested by the geometric external forms and is also confirmed by X-ray diffraction patterns. However, it has been necessary to assume various structural imperfections to explain many important experimental properties of solids. The most important defects are a) interstitial ions, b) vacant lattice sites, c) impurities, and d) dislocations.

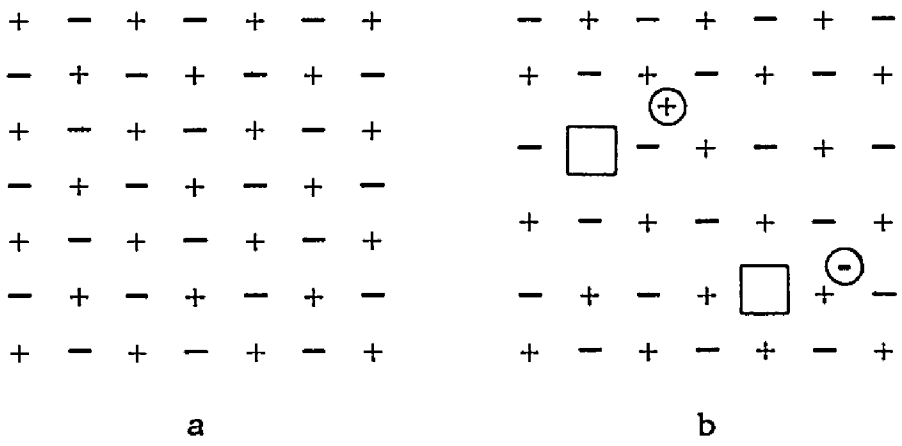

Figure 6

Two Dimensional Representation of a Polar Crystal: a) Containing No Defects, b) with Interstitial Ions

Figure 6a shows a two dimensional representation of a polar crystal containing no defects. In Figure 6b is a crystal with two types of interstitial ions. One of them, M^+, is formed by the removal of a cation from its normal lattice site and placed in an inter-lattice position; the other, X^-, is formed when an anion is similarly displaced.

By removing either of these ions, a vacant lattice site is created, either an anion or a cation vacancy. This mechanism of defect formation is called the Frenkel mechanism and the dual imperfection, the interstitial ion together with the vacancy is known as Frenkel defect.

Vacant lattice sites may be formed in another way, without the production of interstitial ions. This defect is shown in Figure 7 where both the cations and anions are removed from the interior of the crystal and added to the surface to form a new layer of the crystal. This dual imperfection consisting of a cation and an anion vacancy is called a Schottky defect.

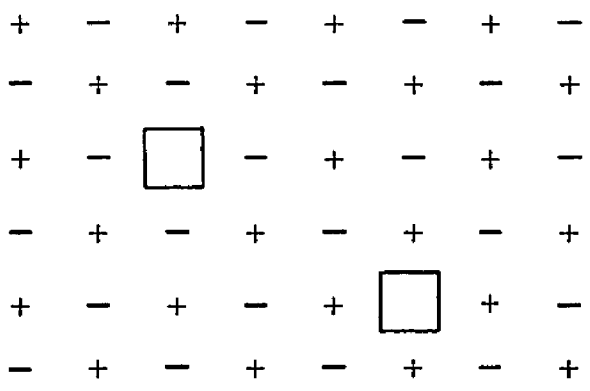

Figure 7

Vacant Lattice Sites

By incorporating chemical impurities into the crystal, vacancies and interstitial ions can also be produced. A two dimentional polar crystal composed of monovalent ions with some of the cations being replaced at random by divalent positive ion impurities is shown in Figure 8. In order to preserve the electrical neutrality of the crystal as a whole, either an extra negative ion must be incorporated interstitially or a positive ion vacancy must be formed at a

lattice point.

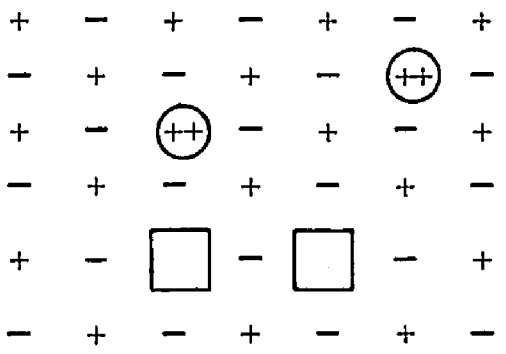

Figure 8.

Cation Impurities Incorporated in a Crystal Lattice

Vacancies and interstitial ions are local regions of unbalanced charge in the crystal. Thus a cation vacancy bears an effective negative charge and an anion vacancy an effective positive charge. This causes an electrostatic attraction of two defects which leads to the formation of a double vacancy or a pair. The binding energy of such a pair is reasonably large, so a substantial concentration of such pairs is expected, Figure 9.

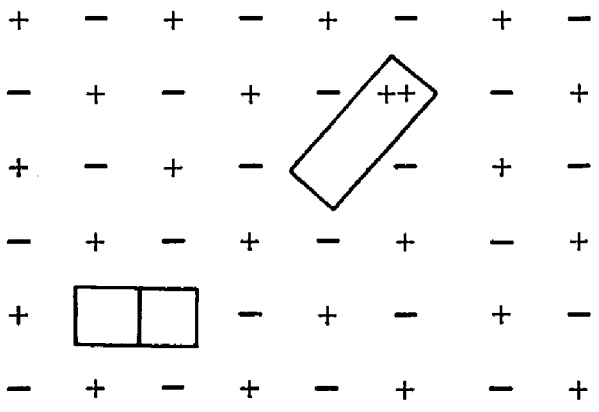

Figure 9.

Pair Formation of Defects in a Crystal Lattice

Similarly the divalent impurity cation shown in Figure 9 has an effective single positive charge while the cation vacancy has an equal negative charge. The impurity cation M would be expected to attract the hole to form a complex.

A dislocation is an imperfection in a crystal associated with the misregistry of the lattice in one part of the crystal with that in another part. There are two principal kinds of dislocations: edge and screw dislocations. An edge dislocation may be considered as being formed by the insertion of an extra plane of atoms part way into the crystal as is shown in Figure 10.

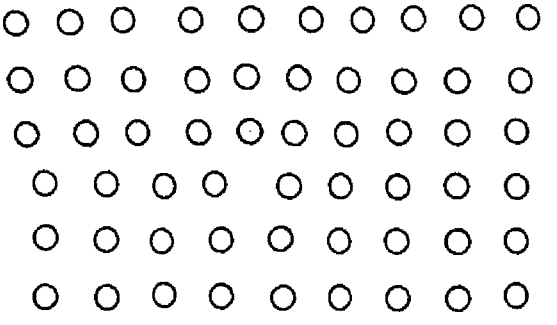

Figure 10

An Edge Dislocation

In screw dislocation a distortion of the lattice without a specific slip plane into a helical pattern is observed. Dislocations in general have partly edge and partly screw character.

Because of the effective charge on vacancies, interstitial ions, and impurity ions, they attract binding electrons and positive holes that have been released in the crystal by some process such as irradiation by x-rays. If an interstitial cation traps an electron, it forms an interstitial

atom. A positive hole might also be trapped by an interstitial anion to form an interstitial atom.

b. Radiation Induced[89] Imperfections

When a perfect crystal is treated with energetic radiation, defects and imperfections are produced. The spatial arrangement of these defects left after the irradiation has ceased is known as radiation damage. Those defects that are inherent in the crystal (discussed in the previous section) are also produced as a result of irradiation of the crystal. Point defects[86] such as vacancies, interstitials, Frenkel defects (interstitial-vacancy pair) and Schottky defects (a pair of vacancies of opposite sign) occur as a result of irradiation of the crystal. It is also possible for point defects to interact with each other and to cluster to form a line defect. Under more extreme conditions large concentrations of point defects aggregate together to form dislocations.

The number of impurity point defects introduced by nuclear transmutation and by the fission process are insignificant by comparison with the number of Frenkel and Schottky defects. Thus in an irradiated crystal there is a large number of defects, inherent and radiation-induced, compared to the number of radioactive atoms produced.

E. Some Properties of ^{32}P

1. Production

Phosphorus-32, a radioactive isotope of phosphorus, does not occur in nature. The first artificial production is attributed to Fermi and his co-workers.[90,91] They were able to obtain ^{32}P by two methods: ^{32}S (n,p)^{32}P and ^{35}Cl (n,α)^{32}P. Since then other nuclear reactions have been used to produce ^{32}P. Reactions such as ^{31}P (d,p)^{32}P, ^{31}P (n,γ)^{32}P,

$^{29}Si(\alpha,p)^{32}P$, $^{30}Si(^{3}He,p)^{32}P$, $^{32}S(d,2p)^{32}P$, $^{34}S(d,\alpha)^{32}P$, $^{28}S(\alpha,\gamma)^{32}P$, $^{35}Cl(d,p\alpha)^{32}P$ and $^{37}Cl(\gamma,\alpha n)^{32}P$, have all been investigated.[92-100] The most often studied reactions are the $^{32}S(n,p)^{32}P$, $^{35}Cl(n,\alpha)^{32}P$ and $^{31}P(n,\gamma)^{32}P$ reactions. In the present work the (n,α) reaction has been used.

The cross section for this reaction rises from about 10 mb at a neutron energy of 3 Mev and to about 65 mb at E_n = 4 Mev.[101] At 14 Mev it is 100 $\pm$ 20 mb[102], at E_n = 14.5 Mev 191 $\pm$ 30 mb[103] and at E_n = 14.8 Mev it is 122 $\pm$ 56 mb.[104]

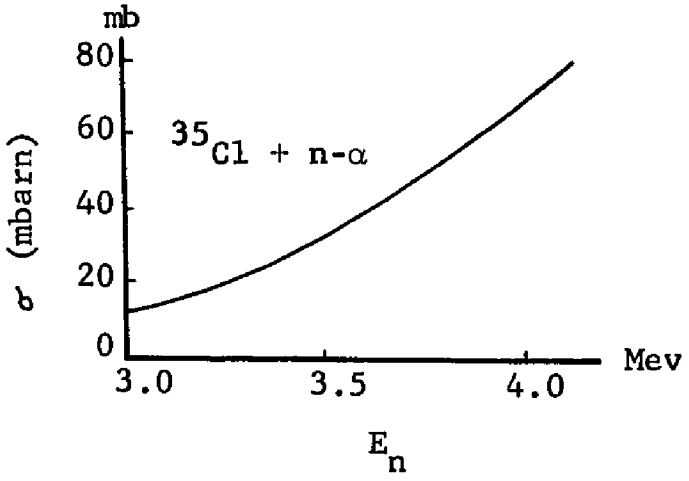

Figure 11

Cross Section of $^{35}Cl(n,\alpha)^{32}P$ Reaction as a Function of Neutron Energy in the Range 3.0-4.0 Mev.[101]

2. Decay Scheme

Phosphorus-32 decays to ^{32}S which is naturally stable. It has a half-life of 14.3 days. ^{32}P is a pure negatron emitter. The maximum beta energy for this decay is 1.71 Mev. The decay scheme is shown in Figure 12.[105]

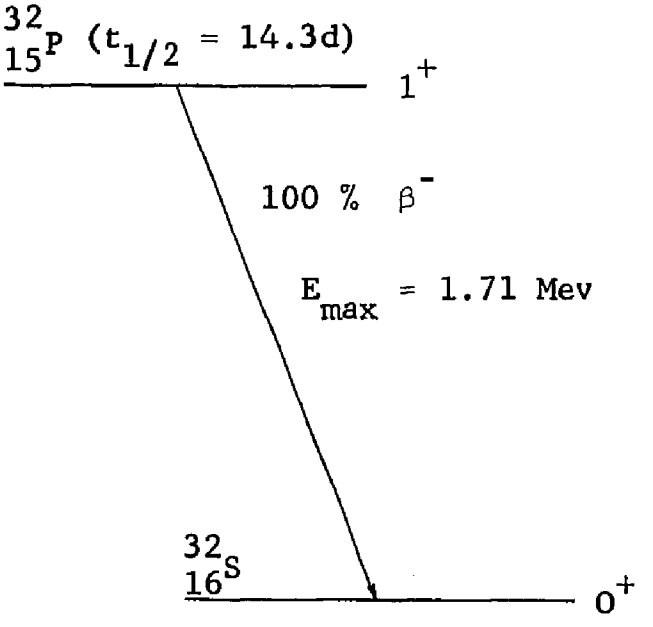

Figure 12

Decay Scheme of ^{32}P

F. Isotopic Exchange Between Phosphorus Oxyanions

It is important that no exchange should occur between the different species of phosphorus oxyanions considered in this thesis if the quantitative results are to be attributed to the original recoil process. Various isotopic exchange studies have been done by others on the oxyanions of phosphorus. These were all carried out in aqueous solution. As shown below no exchange of phosphorus between the three forms of phosphorus, phosphate, phosphite, and hypophosphite is expected to occur under any of the experimental conditions used in this work.

An exchange of phosphorus between ortho-phosphate and ortho-phosphite species was attempted by Wilson[106] by a process of reversible reactions, first forming hypophosphate and subsequent hydrolysis of it.

$$H_3{}^{32}PO_4 + H_3PO_3 \not\rightleftharpoons H_4P_2O_6 + H_2O \not\rightleftharpoons H_3PO_4 + H_3{}^{32}PO_3$$

No measurable exchange was found in this system either in acid or alkaline solutions at a temperature range of 20-100°C. Thus it was concluded that the hydrolysis of hypophosphoric acid is irreversible.

Direct exchange of phosphorus between ortho-phosphate and ortho-phosphite and between ortho-phosphate and ortho-hypophosphite was also attempted, but none was found either in acid or alkaline solutions at a temperature range of 20-380°C.[107]

$$H_3{}^{32}PO_4 + H_3PO_3 \not\rightleftharpoons H_3PO_4 + H_3{}^{32}PO_3$$

$$NaH_2{}^{32}PO_4 + NaH_2PO_2 \not\rightleftharpoons NaH_2PO_4 + NaH_2{}^{32}PO_2$$

Brodskii, Strazhesko and Chervgatsova found no exchange of phosphorus between ortho-phosphite and ortho-hypophosphite species, either in acid or neutral solutions at temperatures up to 70°C.[108]

$$H_3{}^{32}PO_2 + H_3PO_3 \rightleftharpoons H_3PO_2 + H_3{}^{32}PO_3$$

$$KH_2{}^{32}PO_2 + K_2HPO_3 \rightleftharpoons KH_2PO_2 + K_2H{}^{32}PO_3$$

III. EXPERIMENTAL DETAILS

A. Preparation of Samples

Fisher certified reagent grade alkali chlorides were used without further purification, except that they were annealed at 100°C for two hours to drive off water of absorption. Lithium chloride, especially, is highly hygroscopic. About 200 mg quantities were put into quartz tubes (size: 0.5 x 4 cm) and were vacuum-sealed. (1 mm Hg)

B. Irradiation of Samples

The quartz sample tubes were individually wrapped in aluminum foil and were placed in snap-cap polyethylene vials which were then heat-sealed. Samples of the same alkali chloride were always irradiated simultaneously in the same vial. Irradiations were carried out at the U.S. Army Materials and Mechanics Research Reactor, Watertown, Mass. The neutron flux was about 2×10^{12} $n/cm^2/sec$, the gamma flux about 140 megarads/hour and the ambient temperature 100°C. Irradiation time was 5 minutes. After irradiation the samples were kept at room temperature in darkness for at least one week pending subsequent treatment.

C. Photo-annealing of Samples

An Aminco grating monochromator by American Instrument Co., Inc. was used for the photo-annealing of alkali chlorides. A xenon lamp was used as the source of the green light. A simple block diagram of the apparatus is shown in Figure 13.

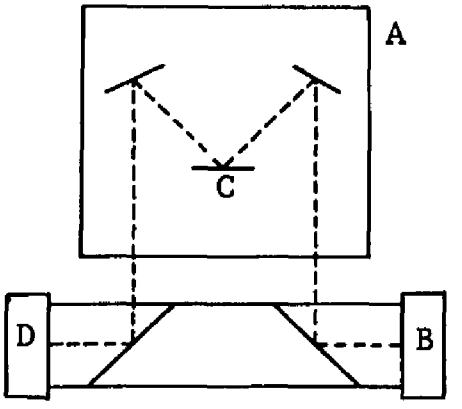

Figure 13

Apparatus for Photo-annealing
A- Monochromator, B- Light source, C- Gratings, D-Cell (for samples)

The wavelength of the light was adjusted to 552 nm, and the intensity of the lamp was measured before each illumination with a short wave UV-meter. Intensity was constant at 165 $w/cm^2 \pm 5$, and no corrections for variation were necessary. Each irradiated sample was transferred into a silica cell and illuminated for a given period of time. Care was taken to avoid premature and post-annealing exposure of the samples to light. The aluminum foil wrapper was taken off in the dark and the quartz sample tube was transferred to the silica cell wrapped with cardboard. This was further wrapped with black cloth and carried over to the monochromator. The silica cell was placed in the instrument in the dark. After illumination, the same precautions were taken. The quartz sample tube was broken and the sample was dissolved in the carrier solution under the black cloth in the dark.

D. Analysis of the Samples

The distribution of the ^{32}P radioactivity obtained upon dissolution of the irradiated and annealed samples was determined according to the scheme shown in Figure 14. Approximately 200 mg of sample was dissolved in 5 ml of an aqueous solution containing 61 millimoles each of $Na_3PO_4 \cdot 12H_2O$, $Na_2HPO_3 \cdot 5H_2O$ and $NaH_2PO_2 \cdot H_2O$. For the reasons outlined in the discussion section, phosphorus in the pentavalent state, P (V), is expected to stabilize in water solution under these conditions as ortho-phosphate, (PO_4^{3-}); phosphorus in the trivalent state, P (III), as phosphite, (PO_3^{3-}), and phosphorus in the univalent state, P (I), as hypophosphite, (PO_2^{3-}).

The solution was diluted with water and divided into three equal aliquots, each about 15 ml. Phosphate, (PO_4^{3-}), was precipitated from the first aliquot as $NH_4MgPO_4 \cdot 6H_2O$ as described below. (There is no interference by other phosphorus oxyanions under the conditions used here). Phosphite, (PO_3^{3-}), in the second aliquot was oxidized to phosphate as described below, and the total phosphate precipitated as $NH_4MgPO_4 \cdot 6H_2O$. In the third aliquot, both phosphite and hypophosphite, (PO_2^{3-}), were oxidized to phosphate (described below) before precipitation as $NH_4MgPO_4 \cdot 6H_2O$.

1. Oxidation of Phosphite to Phosphate

Phosphite was oxidized to phosphate by the method of Jones and Swift[109] except that ammonium acetate buffer was used to maintain pH $\sim$7. The second aliquot was made neutral by the addition of dilute hydrochloric acid. Approximately 10 ml of 3 M ammonium acetate solution was added, thus preventing the oxidation of hypophosphite to phosphate which takes place in acidic solutions. About 1.5 ml ($\sim$10% excess)

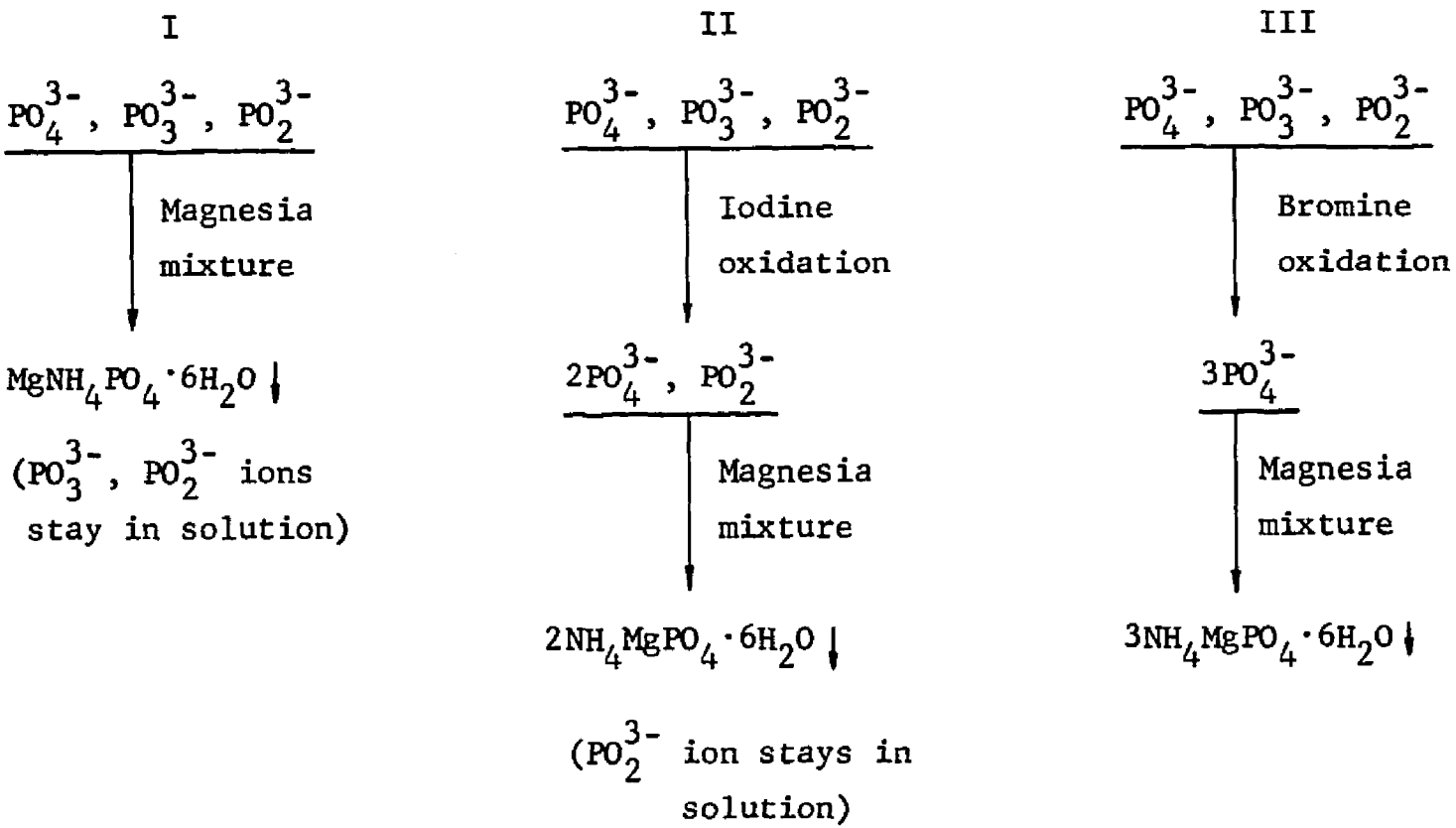

Figure 14

Separation Scheme of Phosphorus Oxyanions

of 0.1 M iodine solution (12.7 g I_2 and 40 g KI dissolved in enough water to give 1 ℓ solution) was added to the radioactive solution. The flask was gently swirled and placed in the dark for one hour. The oxidation takes place according to the following equation by Jones and Swift:

$$H_3PO_3 + H_2O + I_3^- = H_3PO_4 + 2H^+ + 3I^- \text{ (neutral solution)}$$

2. Oxidation of Hypophosphite to Phosphate

Hypophosphite and phosphite were both oxidized to phosphate by the method of Schwicker.[110] The oxidation proceeds as shown below:

$$2BrO_3^- + 5PO_2^{3-} + 2H^+ = 5PO_3^{3-} + Br_2 + H_2O$$

$$2BrO_3^- + 5PO_3^{3-} + 2H^+ = 5PO_4^{3-} + Br_2 + H_2O$$

To the third aliquot, 1-2 ml of a solution prepared by dissolving 2 g of KBr in 100 ml of 0.1 M $KBrO_3$ was added. Then successively 5 ml of 2 M H_2SO_4 and excess (25-30 ml) of 0.1 M $KBrO_3$ were added. The solution was heated just to boiling and when bromine appeared the solution was set aside for 30 minutes. After completion of the oxidation the bromine formed was boiled off and the solution left to cool.[111]

3. Determination of Phosphate as $NH_4MgPO_4 \cdot 6H_2O$

Phosphate was precipitated as $NH_4MgPO_4 \cdot 6H_2O$[111] from each of the above three solutions in the following way. Three ml of concentrated HCl solution and a few drops of methyl red indicator were added to each of the solutions. About 0.7 ml of magnesia mixture (prepared by dissolving 50 g $MgCl_2 \cdot 6H_2O$ and 100 g NH_4Cl in 500 ml water, NH_4OH added in slight excess,

allowed to stand overnight, made just acid with HCl and diluted to 1 liter) was added by pipette to the first, twice as much to the second and thrice as much to the third solutions. Care was taken to avoid adding more than twice as much magnesia mixture as there was phosphate present to prevent the coprecipitation of ammonium phosphate and magnesium phosphates which alter the chemical composition of the precipitate obtained. Concentrated ammonia (14.8 M) solution was added dropwise slowly while stirring the solution vigorously until the indicator turned yellow. Then 5 ml concentrated ammonia solution was added in excess. The solution was allowed to stand in a cool place overnight to insure complete precipitation.

4. Mounting of $NH_4MgPO_4 \cdot 6H_2O$

The model PM-5 sample preparation set by Nuclear-Chicago Corporation was used to filter and mount $NH_4MgPO_4 \cdot 6H_2O$ precipitates (see Figure 15). The steel filter discs served as a planchet so that the filtered, dried sample was already mounted for insertion into the counter without further manipulation. The filter disc was coated with about 10 mg of Celite by adding 5 ml of 0.2% by weight suspension to the funnel. This was filtered by suction, washed with distilled water, then with three 10 ml portions of 95% ethyl alcohol; this procedure serves to remove most of the adhering water. Finally it was washed with 5 ml portions of anhydrous ether. Then air was drawn through the funnel for 10 minutes. The disc with the Celite coating was removed and allowed to stand in a desiccator for 20 minutes. It was weighed with a Mettler balance accurate to hundredths of a mg.

The disc was remounted and the solution containing the $NH_4MgPO_4 \cdot 6H_2O$ precipitate was transferred to the funnel

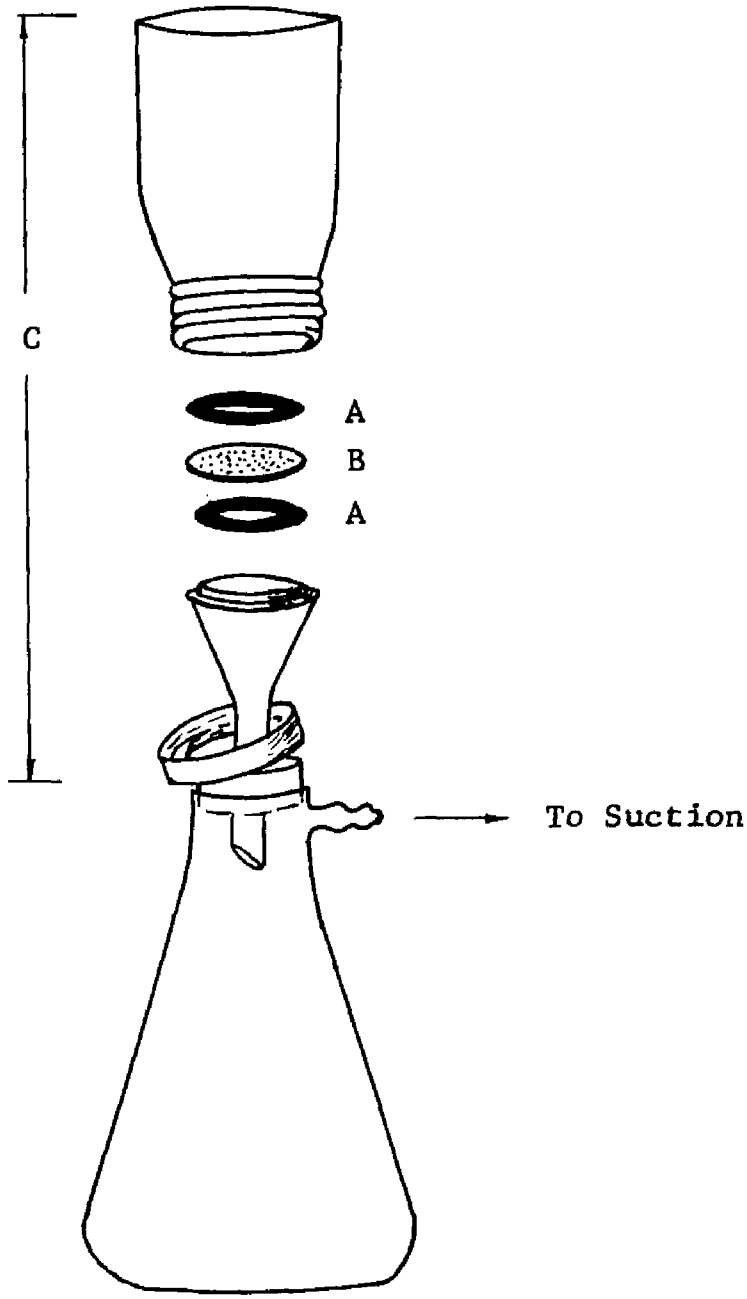

Figure 15

Filtration Apparatus: A. Plastic Rings, B. Porous Metal Disc, C. Chimney-Funnel Set-up

and deposited on the Celite. The precipitate was washed with 10 ml portions of 0.8 M ammonia solution until a few ml of the filtrate gave no test for chloride when acidified with dilute nitric acid and treated with 0.3 M silver nitrate solution. Then it was washed, dried and weighed in the same manner as above.

E. Experiment on Constant Specific Activity

A test experiment was run to check whether reprecipitation of $NH_4MgPO_4 \cdot 6H_2O$ in the above procedure was necessary to obtain a constant specific activity of ^{32}P.

A sample of radioactive LiCl was dissolved in a 5 ml solution containing 61 millimoles of each of PO_4^{3-}, PO_3^{3-} and PO_2^{3-} ions. PO_3^{3-} and PO_2^{3-} ions were oxidized to PO_4^{3-} by bromine and $NH_4MgPO_4 \cdot 6H_2O$ precipitated. Next day the precipitate was filtered, washed and dried as described above and counted. Then it was dissolved in 0.1 N HCl solution and $NH_4MgPO_4 \cdot 6H_2O$ was reprecipitated and left overnight to insure complete precipitation. It was filtered, washed and dried and counted the next day. The results are tabulated below:

Table I

Change of Specific Activity as a Function of Weight

Number of Precipitations	Count Rate* (c/m)	Weight (mg)	Specific Activity (c/m/mg)
1	621 ± 3.6	223	2.78 ± 0.016
2	618 ± 3.6	218	2.79 ± 0.017

*Count rate was corrected both for background and time of decay.

The results indicate that the change in specific activity is negligible. Thus reprecipitation of $NH_4MgPO_4 \cdot 6H_2O$ in the above procedure was not necessary.

F. Measurement of Radioactivity

Radioactivity measurements were done on a Beckman Widebeta II Planchet Counting System (a methane flow counter). All measurements were made with the count mode at "Net", plateau point at "Operate" and analyzer mode at "Beta Plateau".

Each sample was placed in a copper sample pan and then transferred into a specially constructed plastic planchet holder. An absorber of 39.1 mg/cm thickness was used to eliminate ^{35}S activity. Each sample was counted for 50 min. The background was counted with the absorber on before the sample count, using a non-radioactive $NH_4MgPO_4 \cdot 6H_2O$ prepared exactly the same way as the samples. Corrections were made for the background.

It was not necessary to make dead time corrections. The instrument has a resolving time of 0.5 μs, equivalent at 10^6 cpm, using live timing. In this work no count rate exceeded 650 cpm.

G. Calibration for Self-Absorption

The measured radioactivities were corrected for self-absorption using the self-absorption curve shown in Figure 19. The self-absorption corrections also include the effects of backscattering and sidescattering. The self-absorption curve was obtained as described below.

A few drops of radioactive-carrier-free phosphoric acid solution were added to a portion of carrier solution, 0.061 molar in $Na_3PO_4 \cdot 12\ H_2O$. Various volumes of this solution shown in Table II were pipetted into beakers and the

Table II

Self-absorption: Change of Specific Activity as a Function of Weight

Volume of Carrier Soln. (ml)	Magnesia Mixture (ml)	Measured Wt. $NH_4MgPO_4 \cdot 6H_2O$ (mg)	Measured Count Rate (cpm)	Measured Specific Activity (cpm/mg)
1	0.4	15.7	491 ± 3	31.3 ± 0.2
"	"	12.0	399 ± 3	33.3 ± 0.3
"	"	16.0	490 ± 3	30.7 ± 0.2
2	0.8	31.8	951 ± 4	29.9 ± 0.1
"	"	32.1	995 ± 4	31.0 ± 0.1
"	"	31.9	949 ± 4	29.7 ± 0.1
3	1.2	49.4	1,498 ± 5	30.4 ± 0.1
"	"	49.1	1,492 ± 5	30.4 ± 0.1
"	"	48.2	1,495 ± 5	31.1 ± 0.1
5	2.0	78.8	2,382 ± 7	30.2 ± 0.1
"	"	81.4	2,405 ± 7	29.5 ± 0.1
"	"	81.0	2,420 ± 7	29.9 ± 0.1
7	3.0	114.1	3,458 ± 8	30.3 ± 0.1
"	"	113.8	3,385 ± 8	29.8 ± 0.1
"	"	110.8	3,318 ± 8	30.0 ± 0.1

Table II cont.

Volume of Carrier Soln. (ml)	Magnesia Mixture (ml)	Measured Wt. $NH_4MgPO_4 \cdot 6H_2O$ (mg)	Measured Count Rate (cpm)	Measured Specific Activity (cpm/mg)
10	4.0	164.1	4,663 ± 10	28.4 ± 0.1
"	"	165.0	4,655 ± 10	28.2 ± 0.1
"	"	164.7	4,737 ± 10	28.8 ± 0.1

volume of the solution in each beaker was adjusted to 10 ml by adding distilled water. The indicated amount of magnesia mixture was added to each. From this point on, the same precipitation and mounting methods were used as for the sample analysis. The precipitates were weighed and counted, and the specific activity was determined in each case. The data are shown in Table II.

H. Calculation of Distribution of ^{32}P Radioactivity

The activity of each precipitate was counted. Corrections for background, decay and self-absorption were applied to each. The activity obtained from the first aliquot gave the amount of radioactive phosphorus in the P (V) oxidation state, because only PO_4^{3-} ion was precipitated as $NH_4MgPO_4 \cdot 6H_2O$ from the first. The second gave the sum of P (V) and P (III) activities, PO_3^{3-} being oxidized to PO_4^{3-} before $NH_4MgPO_4 \cdot 6H_2O$ precipitation and the third gave the total ^{32}P activity, because both PO_3^{3-} and PO_2^{3-} were oxidized to PO_4^{3-} and all three were precipitated as $NH_4MgPO_4 \cdot 6H_2O$.

To obtain the specific activity for each fraction the following equations were used:

$$I = \frac{\text{Count Rate}_{(1)}\ (\text{cpm})}{\text{Weight}_{(1)}\ (\text{mg})} = \text{cpm/mg}$$

$$II = \frac{\text{Count Rate}_{(2)}\ (\text{cpm})}{\text{Weight}_{(2)}\ (\text{mg})} \times 2 = \text{cpm/mg}$$

$$III = \frac{\text{Count Rate}_{(3)}\ (\text{cpm})}{\text{Weight}_{(3)}\ (\text{mg})} \times 3 = \text{cpm/mg}$$

The multiplication factors, 2 and 3 in the second and the third equations successively, were used to take into account the dilution due to the use of twice and thrice as much $NH_4MgPO_4 \cdot 6H_2O$ as in the first fraction.

Percent distribution of ^{32}P in its three oxidation states was obtained by the following formulas:

$$P\ (V) \qquad \frac{I}{III} \times 100$$

$$P\ (III) \qquad \frac{II-I}{III} \times 100$$

$$P\ (I) \qquad \frac{III-II}{III} \times 100$$

II is the sum of the specific activities of P (V) and P (III). III is the sum of all three specific activities. P (V) is obtained directly from I, P (III) and P (I) are the differences II-I and III-II, respectively.

I. Statistical Analysis

When the averages of the data points at the same annealing time were plotted, considerable changes were recorded from the horizontal straight line which would have been obtained in the case of no annealing. Moreover, these changes were in the same direction at a given annealing time. This is a strong indication that some annealing process occurred. However, a statistical analysis was carried out to investigate further the nature of the deviations from the horizontal straight line.

A computer program was used to find out the best fitting curve. The program makes the least squares approximations where the sum of the squares of the deviations from

the fitted polynomial is a minimum.

$$\sum_{i=1}^{N}(y-\bar{y})^2 = \min.$$

The method of the statistical analysis used here is called the analysis of the variance. A hypothesis is made such as a straight line approximation for a given set of data and then it is tested and F-values obtained. The level of confidence in that hypothesis is found in Tables of F-values.[112-114] The hypothesis can be varied. In our case polynomials of from degree 1 to 4 were tested successively. F is the ratio of σ_1^2 to σ_2^2, independent mean squares estimating a common variance and based on n and m degrees of freedom, respectively. F(F) is a function of gamma function and gives percentage confidence level corresponding to an F-value at known n and m degrees of freedom.

$$F(F) = \int_0^F \frac{\Gamma\left(\frac{m+n}{2}\right)}{\Gamma\left(\frac{m}{2}\right)\Gamma\left(\frac{n}{2}\right)} m^{\frac{m}{2}} n^{\frac{n}{2}} x^{\frac{m}{2}-1} (n+mx)^{-\frac{m+n}{2}} dx.$$

The program is listed in the Appendix.

IV. RESULTS

The percent distributions of ^{32}P activity in each of the three oxidation states, P (V), P (III), and P (I) are given in Tables III, IV and V for lithium, sodium and potassium chloride, respectively. Each percentage is the mean of at least two independent determinations with plus or minus the average deviation from this mean. The activity in each oxidation state has been corrected for self-absorption (which includes sidescattering and backscattering effects). The absorption curve shown in Figure 19 gives a negative slope, indicating the absorption of β^- particles by the sample itself as the weight of the sample is increased. The radiochemical purity was checked with half-life determinations. A sample of each of lithium, sodium and potassium chloride was treated as in the photo-annealing experiments and was counted at intervals for about two half-lives. The experimental half-life of 14.3 days agrees quite well with the theroretical value of 14.295 days. (Figure 20)

The results of photo-annealing experiments are plotted. Figures 16, 17 and 18 show the percent distribution of ^{32}P activity as a function of photo-annealing time. The curves corresponding to the same phosphorus oxyanion show marked similarities. At zero annealing the percent P (V) is about the same for all three chlorides, $47.2 \pm 1.2\%$. The other oxidation states, however, have different values.

Cifka obtained 65.6, 13.1 and 21.3 for P (V), P (III) and P (I) in KCl. Respective values for KCl obtained in this work are 48.4, 30.7 and 21.0 and show an increase of P (III) fraction at the expense of P (V). This might be due to the

presence of a larger concentration of F-centers in these samples, the reducing action of different and/or more impurities or the difference in reactor conditions.

Babtista, Newton and Robinson obtained 24.0, 10.9 and 65.1% for P (V), P (III) and P (I), respectively; almost complete reversal of Cifka's values. They used single crystals of KCl obtained by the Stockbarger method after purification by zone-refining. They concluded that the presence of impurities such as OH and CO_3 ions in the crystal tends to oxidize the recoils to higher oxidation states; also defects such as dislocations and anion vacancies act as traps for electrons, oxidizing phosphorus to the P (V) fraction.[14]

Table III

Distribution of ^{32}P Activity Among P(V), P(III) and P(I) in LiCl

Time of Annealing	% P(V)	% P(III)	% P(I)
0 min.	47.3 ± 2.3	19.9 ± 2.0	32.8 ± 2.4
2 "	46.4 ± 2.5	16.8 ± 2.5	36.8 ± 1.4
5 "	47.0 ± 2.8	18.5 ± 0.9	34.5 ± 2.8
10 "	40.2 ± 0.2	21.1 ± 1.3	38.7 ± 1.5
20 "	44.5 ± 0.8	16.2 ± 0.5	39.2 ± 0.6
30 "	43.4 ± 0.6	13.9 ± 2.5	42.6 ± 2.3
40 "	45.5 ± 0.1	17.6 ± 0.5	37.0 ± 0.7

Table IV

Distribution of ^{32}P Activity among P(V), P(III) and P(I) in NaCl

Time of Annealing	% P(V)	% P(III)	% P(I)
0 min.	45.8 ± 0.2	11.1 ± 1.1	43.1 ± 1.3
2 "	49.7 ± 1.1	11.5 ± 2.8	39.2 ± 0.5
5 "	47.3 ± 2.2	11.1 ± 2.2	41.7 ± 0.5
10 "	48.2 ± 1.4	7.2 ± 1.0	44.6 ± 1.6
15 "	47.9 ± 2.5	11.5 ± 1.0	40.6 ± 3.7
20 "	49.1 ± 1.1	11.4 ± 0.7	39.5 ± 2.5
30 "	49.9 ± 1.0	12.2 ± 0.1	37.9 ± 0.9
40 "	51.9 ± 2.8	11.0 ± 1.8	37.1 ± 2.9

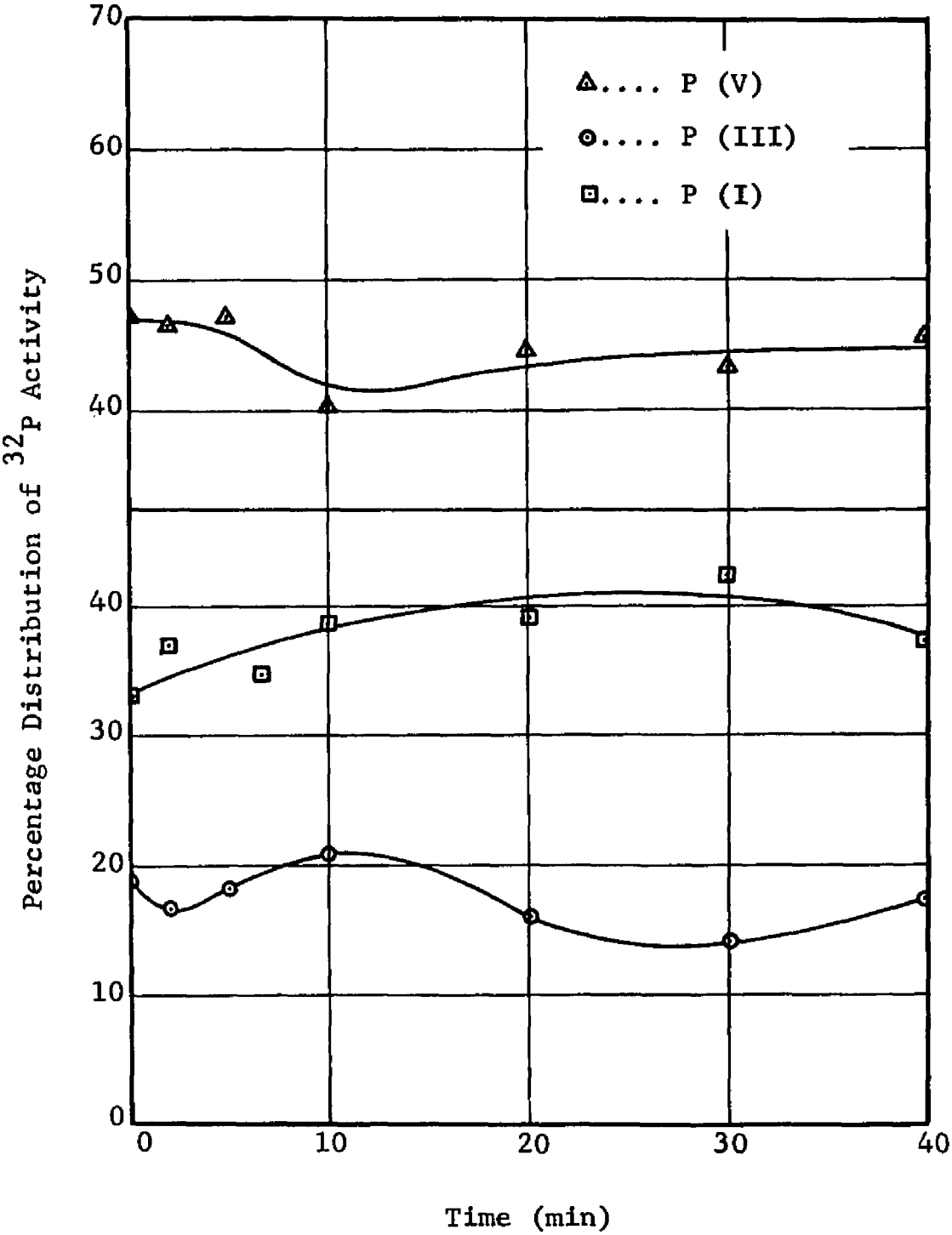

Figure 16

Photo-annealing of ^{32}P in LiCl with 552 nm Light

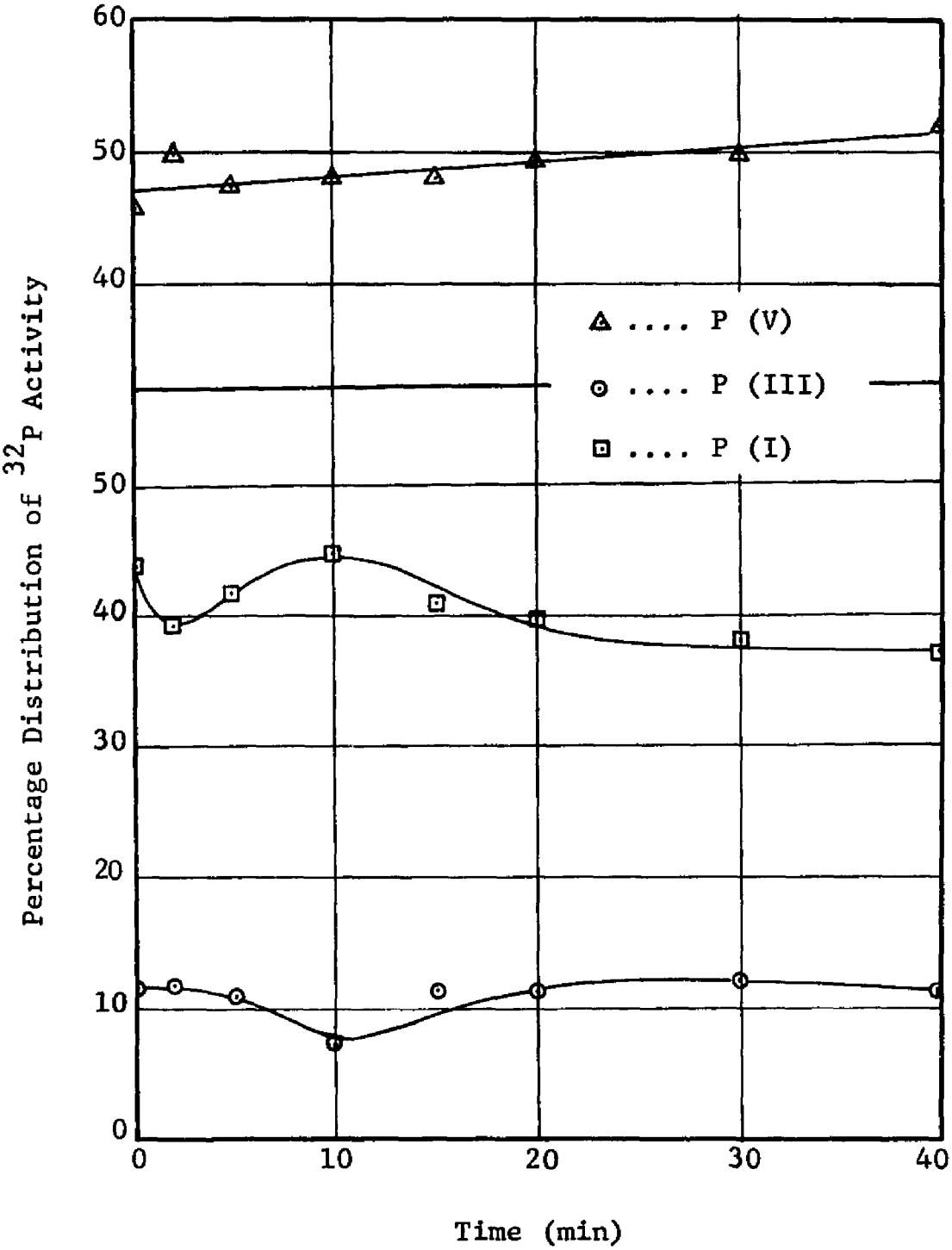

Figure 17

Photo-annealing of ^{32}P in NaCl with 552 nm Light

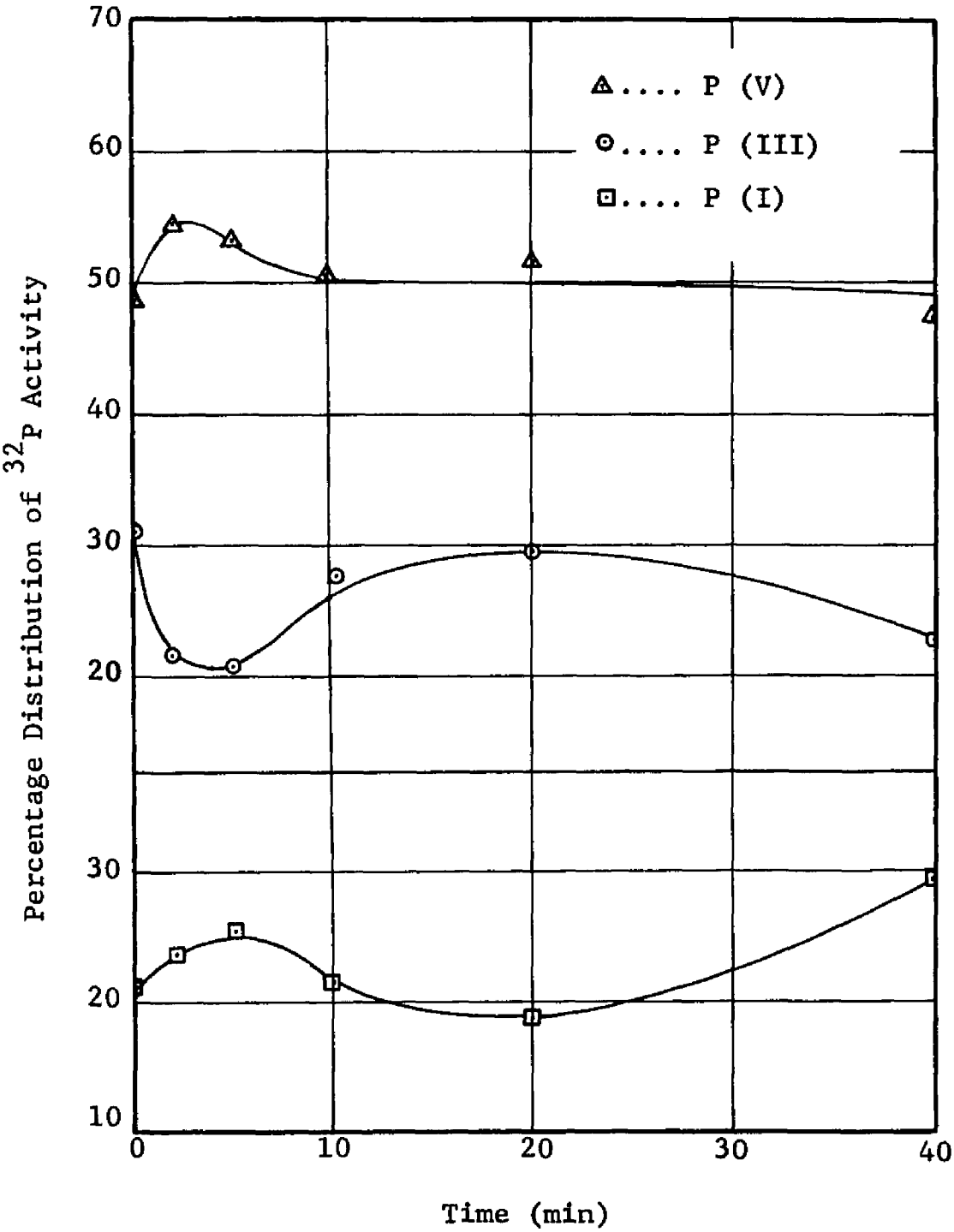

Figure 18

Photo-annealing of ^{32}P in KCl with 552 nm Light

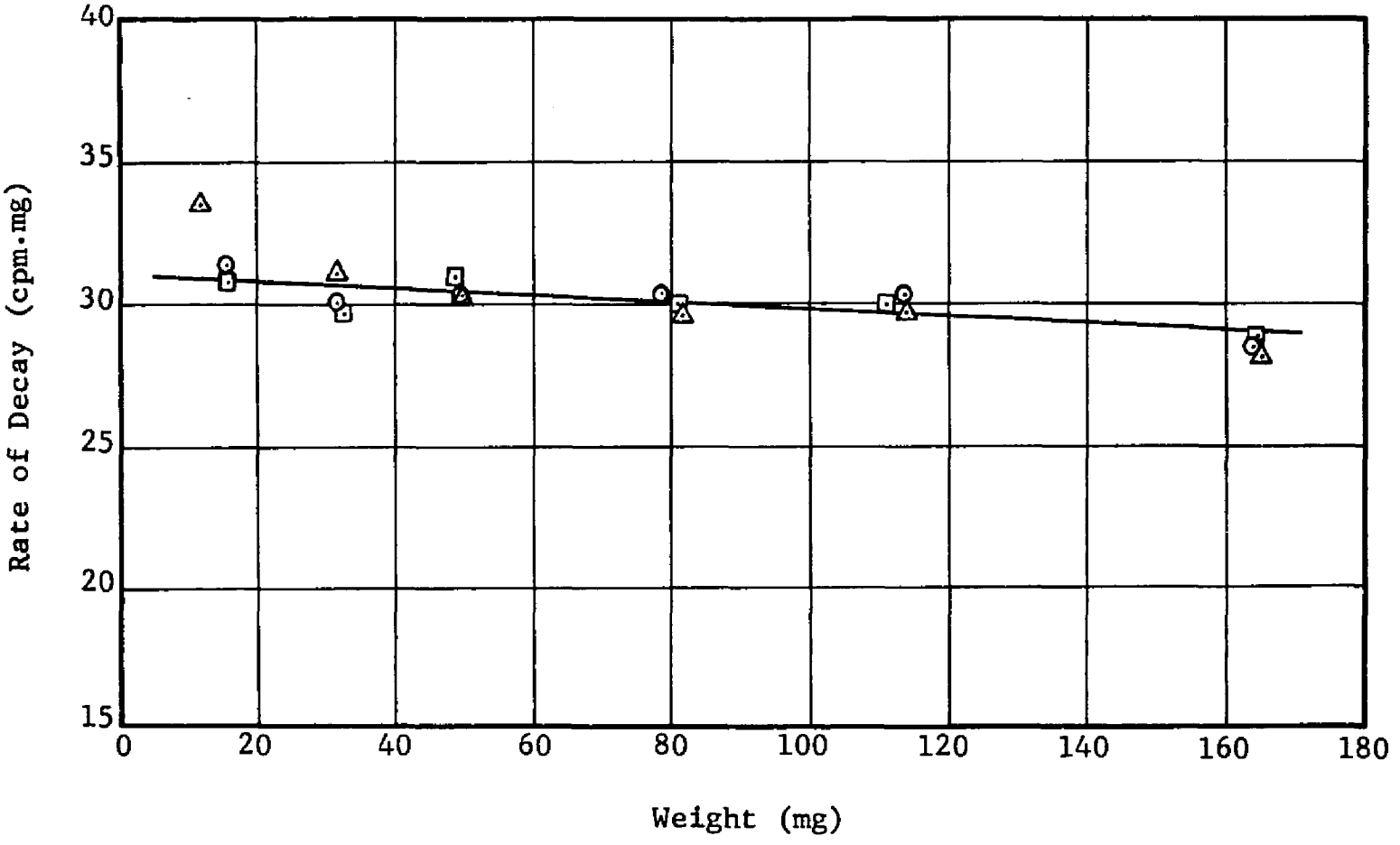

Figure 19

Absorption Curve for $MgNH_4PO_4 \cdot 6H_2O$

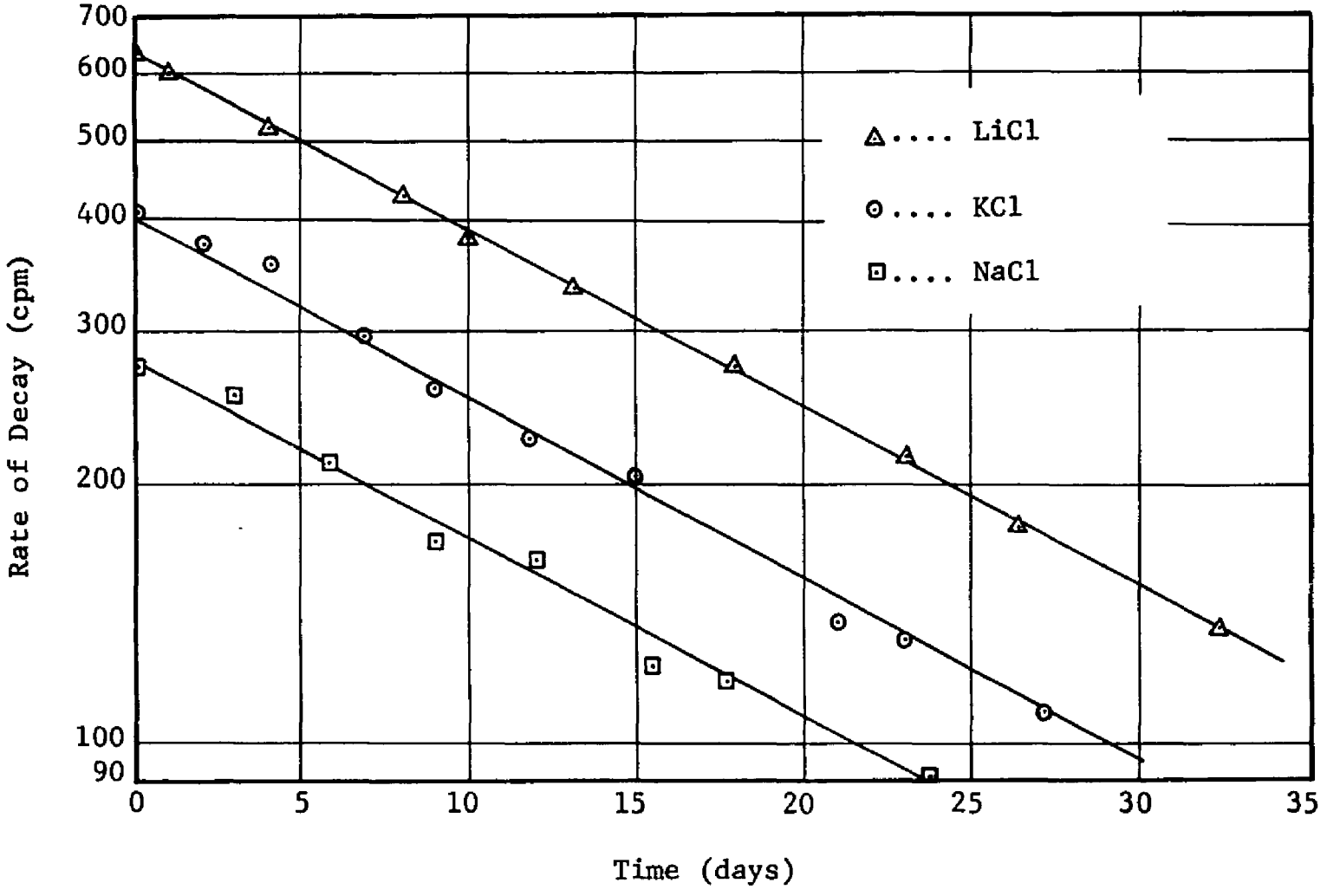

Figure 20

Exponential Decay of ^{32}P in LiCl, NaCl and KCl

The output from the computer program is given in Table VI for each phosphorus oxyanion in each alkali chloride used. Degree of regression represents the degree of polynomial to which the data were fitted. Regression coefficients are the constants in the equation $ax^4 + bx^3 + cx^2 + dx + e = y$. N_1 is the degree of polynomial and N_2 is obtained by the difference of N_1 and the total number of data points for that particular set. The program gives F-values for each of the polynomials tested. The F ratio is defined by

$$F = \frac{\sigma_1^2}{\sigma_2^2}$$

where σ_1^2 and σ_2^2 are independent mean squares estimating a common variance based on N_1 and N_2 degrees of freedom, respectively. F-tables were used to find the corresponding level of confidence expressed as a percentage. It was necessary in some cases to make interpolations or for x less than 50% confidence levels to look up the F-values corresponding to 100-x at exchanged N_1 and N_2 values and take $\frac{1}{F}$ for the x confidence level.

The mean values given in Tables III, IV and V were plotted in Figures 16, 17 and 18. To draw the best fitting curves through the data points, the percent confidence for each polynomial was taken into consideration; the highest was usually accepted for that particular set and the curve was drawn. The choice was difficult in some cases where the percentages were either too close to chose one or all four of them were lower than 90% confidence level. For instance, in the case of P (V) in NaCl the percentages were 99.1, 98.0, 94.0 and 91.3 for the 1st, 2nd, 3rd and the 4th degree polynomials, respectively, all above 90% confidence level. For

P (III) in NaCl again, 47.8, ~20, 83.5 and 72.3% were obtained. These values are too low to rely on any one, so a curve was drawn passing through the experimental points, disregarding the choice of the 3rd degree polynomial. For KCl both the 3rd and the 4th degree polynomials had the highest percentages. However, when these curves were drawn, a maximum or a minimum was obtained between two consecutive points due to lack of enough data points. Since there is no experimental evidence for these humps, they were disregarded at these points and a line with smaller curvature was drawn to fit the points. The beginning of the statistics-suggested curve, where there were enough points to justify the choice, was drawn according to the given equation.

Table VI

Output from Computer Program for LiCl Data

Ion	Regression Coefficients					F-value	Level of Confidence
	a	b	c	d	e		
P (V)				-0.513×10^{-1}	46.004	1.034	68 %
"			0.797×10^{-2}	-0.345	47.104	2.080	84.4 %
"		-0.422×10^{-3}	0.332×10^{-1}	-0.716	47.793	1.702	78.8 %
"	0.242×10^{-5}	-0.611×10^{-3}	0.377×10^{-1}	0.748	47.825	1.192	62.7 %
P (III)				-0.922×10^{-1}	18.861	3.894	93.0 %
"			0.371×10^{-2}	-0.229	19.374	2.242	86.2 %
"		0.745×10^{-3}	-0.409×10^{-1}	0.424	18.159	2.909	92.7 %
"	0.390×10^{-4}	-0.229×10^{-2}	0.312×10^{-1}	-0.951×10^{-1}	18.696	2.389	90.0 %
P (I)				0.155	35.098	7.876	98.8 %
"			-0.121×10^{-1}	0.605	33.419	8.880	99.8 %
"		-0.454×10^{-3}	0.150×10^{-1}	0.206	34.160	6.345	99.4 %
"	-0.533×10^{-4}	0.370×10^{-2}	-0.835×10^{-1}	0.916	33.427	5.285	99.1 %

Table VI cont.

Output from Computer Program for NaCl Data

Ion	Regression Coefficients					F-value	Level of Confidence
	a	b	c	d	e		
P (V)				0.107	46.956	8.406	99.1 %
"			0.305×10^{-2}	-0.116×10^{-1}	47.495	4.615	98.0 %
"		0.328×10^{-4}	-0.238×10^{-2}	0.639×10^{-1}	47.349	2.945	94.0 %
"	-0.332×10^{-4}	0.266×10^{-2}	-0.631×10^{-1}	0.512	46.857	2.432	91.3 %
P (III)				0.225×10^{-1}	10.318	0.458	47.8 %
"			0.193×10^{-2}	-0.528×10^{-1}	10.659	0.434	20 %
"		-0.639×10^{-3}	0.394×10^{-1}	-0.573	11.666	1.958	83.5 %
"	0.279×10^{-5}	-0.856×10^{-3}	0.445×10^{-1}	-0.611	11.707	1.389	72.3 %
P (I)				-0.130	42.719	8.252	99.2 %
"			-0.495×10^{-2}	0.631×10^{-1}	41.845	5.051	98.2 %
"		0.545×10^{-3}	-0.369×10^{-1}	0.507	40.985	4.077	97.8 %
"	0.301×10^{-4}	-0.178×10^{-2}	0.181×10^{-1}	0.100	41.429	3.134	95.8 %

Table VI cont.

Output from Computer Program for KCl Data

Ion	Regression Coefficients					F-value	Level of Confidence
	a	b	c	d	e		
P (V)				-0.923×10^{-1}	52.203	3.516	90.8 %
"			-0.562×10^{-2}	0.133	51.300	2.698	88.0 %
"		0.464×10^{-3}	-0.322×10^{-1}	0.474	50.721	1.894	78.7 %
"	-0.412×10^{-3}	0.284×10^{-1}	-0.562	0.330×10^{1}	48.701	13.527	99.7 %
P (III)				-0.256×10^{-1}	26.047	0.084	22.2 %
"			-0.805×10^{-2}	0.297	24.754	0.532	39.5 %
"		-0.213×10^{-2}	0.114	-0.127×10^{1}	27.418	2.280	88.0 %
"	0.655×10^{-3}	-0.466×10^{-1}	0.957	-0.577×10	30.510	79.301	99.9 %
P (I)				0.120	21.734	2.900	87.6 %
"			0.138×10^{-1}	-0.434	23.952	6.124	98.0 %
"		0.167×10^{-2}	-0.82×10^{-1}	0.796	21.865	14.388	99.9 %
"	-0.243×10^{-3}	0.182×10^{-1}	-0.395	0.247×10	20.794	16.130	99.8 %

V. DISCUSSION

The differences in the initial percentages of the same phosphorus-containing ion in different halides can be attributed to the presence of different amounts and kinds of impurities, and defects initially present in the crystal or formed as a result of irradiation. They cannot be attributed to crystal structure, since these are identical , or to different irradiation conditions, because they were all irradiated at the same reactor for the same length of time for comparison. One cannot say how much the effect of the cation is on the distribution of the oxidation states, since it is not possible to isolate the effects of impurities, and defects from the cation effect. There might be both oxidizing and reducing porcesses occurring at the same time, thus cancelling or minimizing the overall effect.

At zero annealing ^{32}P activity as P (V) ion shows almost the same percentage for all the three alkali chlorides, 47.3, 45.8 and 48.4% for LiCl, NaCl and KCl, respectively. P (III) and P (I) ions have different percentages in different chlorides but exhibit a trend that can be explained by crystal impurity. The percent ^{32}P as P (I) is 21.0 for KCl, 32.8 for LiCl, and 43.1% for NaCl. P (III) ion shows a similar trend in the opposite direction. Since P (V) remains constant in all three there seems to be a trade-off between the other two ions; a decrease in one is accompanied by an increase in the other. In the work of Babtista, Newton, and Robinson, pure and perfect crystals of KCl are shown to be reducing in character, while pure-defective crystals act as oxidizing agents towards recoils and impure-defective crystals are

variable, often reducing.[14] P (I) ion has a higher percentage than the other two in zone-refined KCl samples. KCl doped with OH, CO_2 and CO_3 impurities has a higher percentage of P (V) ion. The presence of these and other oxygen containing impurities result in the formation of higher oxidation states.

In this work, the samples of LiCl, NaCl and KCl contain various amounts of impurities as indicated on the labels of the bottles (Table VII). KCl seems to be the most impure. It has such oxygen-containing impurities, NO_3, PO_4, SO_4 and ClO_4, halide impurities Br and I and some metal impurities Ba, Mg, Ca, Na and Fe. LiCl has oxygen impurities in the form of NO_3 and SO_4 and metal impurities such as Na, K, Ca, Ba, Fe and Pb. NaCl has only ClO_4 and NO_3 and Ca, Mg and Fe. LiCl and NaCl thus have less impurities than KCl. In KCl a smaller percentage of P (I) than P (III) would be expected, since impurities tend to oxidize the recoils. The experimental results confirm this expectation. KCl has 21.0% P (I), lowest among the three chlorides. NaCl has the highest, 43.1%. LiCl is expected to have a similar percentage; however, it is lower, 32.8%. This can be explained by the fact that LiCl is one of the most hygroscopic compounds. Even though care was taken in sample preparation to evaporate the moisture, probably some H_2O was left in the sample. LiCl was previously stored at 100°C for two hours like the rest of the chlorides. It was then put in quartz sample tubes and vacuum-sealed. It was exposed to air during its transfer to the tubes and might easily pick up moisture. There are, of course, OH^- ions in the other chlorides as well, but most probably not as many as in LiCl samples. This might explain the lower percentage of P (I) in LiCl than in NaCl. The presence of OH, CO_3, CO_2 or other oxygen-containing impurities

Table VII

Reported Impurities in
Lithium, Sodium and Potassium Chloride

LiCl

Sulfate	(SO_4)	0.003 %
Calcium	(Ca)	0.004 %
Barium	(Ba)	0.003 %
Iron	(Fe)	0.0003 %
Insoluble Matter		0.01 %
Nitrate	(NO_3)	0.001 %
Heavy Metals (as Pb)		0.0004 %
Potassium	(K)	0.003 %

NaCl

Iodide	(I)	0.000 %
Insoluble Matter		0.000 %
Chlorate and Nitrate (as NO_3)		0.003 %
Nitrogen Compounds (as N)		0.001 %
Phosphate	(PO_4)	0.0000 %
Sulfate	(SO_4)	0.000 %
Calcium, Magnesium and R_2O_3 ppt		0.002 %
Heavy Metals (as Pb)		0.0001 %
Iron	(Fe)	0.00004 %
Potassium	(K)	0.000 %

Table VII cont.

KCl

Barium	(Ba)	0.001	%
Bromide	(Br)	0.005	%
Calcium, Magnesium and R_2O_3 ppt.		0.0025	%
Chlorate and Nitrate (as NO_3)		0.003	%
Heavy Metals (as Pb)		0.00025	%
Insoluble Matter		0.0025	%
Iodide	(I)	0.002	%
Iron	(Fe)	0.00015	%
Nitrogen Compounds (as N)		0.001	%
Phosphate	(PO_4)	0.00025	%
Sodium	(Na)	0.005	%
Sulfate	(SO_4)	0.0005	%

leads to the formation of species such as an oxygen atom or a hydride, H^-, as a result of gamma radiolysis of the impurities during irradiation.[80] These species act as electron traps and thus oxidize the recoil products. The presence of Br or I in the crystal might also yield similar results, but there has been no correlation between specific impurities other than OH, CO_2 and CO_3 and the oxidation states of the recoil, no experimental evidence on the effect of I or Br doped KCl on the distribution of ^{32}P activity. But impurities in general cause oxidation.[14]

Crystal defects, initially present in the irradiated material (explained on pp. 33-37), and radiation-induced defects also act as electron traps leading to oxidized species. Using the terms of Babtista, Newton and Robinson[14], the samples used in these experiments can be characterized as polycrystalline, impure and defective, thus leading to higher oxidation states. The total activity in oxidized species, P (V) and P (III), is 79.1% for KCl, 67.2% for LiCl and 56.9% for NaCl, decreasing with the amount of impurity and defect present. The initial concentration of defects might be different in different chlorides and although the irradiation time and conditions are the same for all the three, not necessarily the same kind and amount of radiation-induced defects are produced due to the initial impurities and defects, certain kind of defects and impurities giving rise to various other defects.

Babtista, Newton and Robinson were never able to obtain zero percent P (V) even in the most perfect and pure crystals.[14] Even though these are highly reducing, this might be due to undetected impurities or radiation-induced defects. Another important factor is the oxidizing character of H_2O. One cannot identify the recoil species as they have formed in the

crystal, but must isolate them after dissolution in aqueous solutions. When carriers were added after the dissolution of irradiated sample, P (III) fraction was increased by 10-20% at the expense of P (I) fraction.[14] This effect arises from the competition between exchange and oxidation reactions between carrier and solvent, respectively. In the experiments described in this thesis, the carriers were added prior to the dissolution of the samples. This minimizes solvent oxidation but never eliminates it.

The annealing curves show some interesting features. The photo-annealing observed here is a continuation of the radiation and thermal annealing that has taken place during irradiation. There is no way of finding the ^{32}P activity distribution at zero annealing. It can be estimated by irradiating the sample for shorter periods of time approaching zero and extrapolating the curve to zero time. However, this is not a very accurate method; the activity will be too low and the detection inaccurate, especially for lower values of irradiation time. Although there have been thermal- and radiation-annealing, no photo-annealing could take place, since all the samples were wrapped with aluminum foil. At the beginning of photo-annealing both oxidizing and reducing processes take place. In LiCl P (III) is reduced to P (I) first, then P (V) is reduced to P (III) and eventually to P (I); however, some of P (III) is oxidized back to P (V) towards the end of annealing. In NaCl there is a net increase of P (V) ion at the expense of P (I). P (I) is first oxidized to P (III), then some of P (III) is reduced back to P (I). In KCl P (III) is both oxidized to P (V) and reduced to P (I) at the same time. There might be competing reactions, F-centers, for instance, reducing the higher oxidation states to lower states and impurities such as oxygen increasing P (III) and

P (V) states. During the illumination of the irradiated material the electrons that were trapped in the negative ion vacancies are released and these electrons act as reducing agents of the recoil species.[13]

$$h\nu + F \rightarrow e^- + \text{Negative ion vacancy}$$

$$e^- + {}^{32}P^{n+} \rightarrow {}^{32}P^{+(n-1)}$$

The released electrons might also be trapped by the impurity ions before they get to the recoil species. The impurities and defects might be competing with the electrons for the recoil species. After some critical time when all the electrons, defects and impurities at some distance apart have moved towards the recoil species, the curves level off. The last stages of NaCl and LiCl curves show that there is a net increase of oxidized fractions P (III) and P (V) and a decrease of P (I). In KCl, however, it is just the opposite. There is a great tendency for both P (V) and P (III) to decrease as P (I) increases. The net effect is one of reduction. This observation can be explained in the following manner. Sodium metal forms a colloidal suspension in NaCl salt, but potassium does not in KCl. When NaCl was irradiated with electrons, sodium was formed and detected by coloration of the crystal. This occurs by the electron attaching itself to a sodium ion which combines with other sodium atoms to precipitate out of the salt.[115] This tendency to colloidal formation is less in KCl. In NaCl the electrons combine with Na ions to form Na atoms. In KCl, however, they combine with negative ion vacancies to form F-centers. Later during annealing, the electrons in KCl are easily released with photons and reduce the recoil species. In NaCl electrons

are permanently tied down and although there might be some F-center produced, the electrons released may not be enough to cancel the oxidizing effects of impurities.

VI. SUMMARY

Phosphorus-32 was produced in this work by the reaction $^{35}Cl(n,\alpha)^{32}P$ in alkali chlorides and the distribution of radioactivity among the three oxidation states, P (I), P (III) and P (V) was studied as a function of photo-annealing time.

The results indicate that both oxidizing and reducing reactions are taking place during photo-annealing. This might be due to the competing reactions of oxidation attributed to the presence of varying amounts of impurities present in the crystal and reduction due to the F-centers produced as a result of irradiation (F-electrons mobilized under the influence of illumination with 552 nm light reduce the recoil species). An equilibrium is reached after some critical time when all the electrons, defects and impurities at some distance apart have moved towards the recoil species.

VII. LIST OF REFERENCES

1. L. Szilard and T. H. Chalmers, Nature, 134, 462 (1934).

2. W. F. Libby, J. Amer. Chem. Soc., 69, 2523 (1947).

3. R. R. Edwards and T. H. Davies, Nucleonics, 2, 44 (1948).

4. I. G. Campbell, in "Advances in Inorganic Chemistry and Radiochemistry", Vol. 5, Emeleus and Sharpe Ed., Academic Press Inc., New York, N. Y., 1963, p. 135.

5. R. Wolfgang, Scientific American, 214, 82 (1966).

6. A. H. W. Aten, Jr., Rec. Trav. Chim. Pays-Bas., 61, 467 (1942).

7. A. H. W. Aten, Jr., Phys. Rev., 71, 641 (1947).

8. R. Caillat and P. Süe, Compt. Rend., 230, 1666 (1950).

9. L. Lidner, Ph.D. Thesis, Univ. Amsterdam, 1958.

10. T. A. Carlsen and W. S. Koski, J. Chem. Phys., 23, 1596 (1955).

11. J. S. Butterworth and I. G. Campbell, Nature, 196, 982 (1962).

12. R. F. C. Claridge and A. G. Maddock, Trans. Faraday Soc., 59, 935 (1963).

13. J. Cifka, Proc. Symposium on Chemical Effects Associated with Nuclear Reactions and Radioactive Transformations, II, IAEA, Vienna, (1965), p. 71.

14. J. L. Babtista, G. W. A. Newton, and V. J. Robinson, Trans. Faraday Soc., 64, 456 (1968).

15. T. Andersen, Experimental Investigations of Chemical Effects Associated with Nuclear Transformations in Some Inorganic Solids, University of Aarhus, Denmark, (1968), p. 10.

16. I. Zvara, Fiz.-Khim. Mekh. Mater., 13, 127 (1959).

17. C. Hsiung, H. Hsiung, and A. A. Gordus, J. Chem. Phys., 34, 535 (1961).

18. J. Cifka, Radiochim. Acta, 1, 125 (1963).

19. E. A. Rudak, and E. I. Firsov, Soviet J. Nucl. Phys., 1, 164 (1965).

20. G. A. Bartholomew, E. D. Earle, and M. R. Gunye, Can. J. Phys., 44, 2111 (1966).

21. D. L. Baulch, and J. F. Duncan, Quart. Rev. (London), 12, 133 (1948).

22. S. Wexler, Phys. Rev., 93, 182 (1954).

23. S. Wexler and G. R. Anderson, J. Chem. Phys., 33, 850 (1960).

24. S. Wexler and T. H. Davies, J. Chem. Phys., 18, 376 (1950).

25. S. Wexler and T. H. Davies, J. Chem. Phys., 20, 1688 (1952).

26. T. A. Carlsen, A. H. Snell, F. Pleasonton, and C. H. Johnson, Proc. Symposium on Chemical Effects of Nuclear Transformations, I, IAEA, Vienna, (1961), p. 63.

27. A. H. Snell and F. Pleasonton, J. Phys. Chem., 62, 1377 (1958).

28. A. H. Snell and F. Pleasonton, Phys. Rev., 111, 1338 (1958).

29. A. H. Snell and F. Pleasonton, ibid., 107, 740 (1957).

30. A. Migdal, J. Phys. (U.S.S.R.), 4, 449 (1941).

31. E. L. Feinberg, ibid., 4, 423 (1941).

32. J. D. McGee, Phil. Mag., 13, 1 (1932).

33. W. Mund, P. C. Capron, and J. Jodogne, Bull. soc. chim. Belges, 40, 35 (1931).

34. R. Serber and H. S. Snyder, Phys. Rev., 87, 152 (1952).

35. J. L. Magee and E. F. Gurnee, J. Chem. Phys., 20, 894 (1952).

36. D. R. Wiles and W. H. Wong, Can. J. Chem., 45, 1813 (1967).

37. P. J. Estrup and R. Wolfgang, J. Amer. Chem. Soc., 82, 2665 (1960).

38. P. J. Estrup and R. Wolfgang, ibid., 82, 2661 (1960).

39. A. A. Gordus and Chi-Hua Hsiung, J. Chem. Phys., 36, 947,955 (1962).

40. J. M. Miller, J. W. Gryder, and R. W. Dodson, J. Chem. Phys., 18, 579 (1950).

41. J. M. Miller and R. W. Dodson, ibid., 18, 865 (1950).

42. L. Friedman and W. F. Libby, J. Chem. Phys., 17, 647 (1949).

43. J. E. Willard, Proc. Symposium on Chemical Effects of Nuclear Transformations, I, IAEA, Vienna, (1961), p. 215.

44. M. Milman, Radiochim. Acta, 2, 180 (1964).

45. P. F. D. Shaw, ibid., 1, 177 (1963).

46. P. F. D. Shaw, ibid., 1, 188 (1963).

47. G. Harbottle and N. Sutin, J. Phys. Chem., 62, 1344 (1958).

48. F. Seitz and J. S. Koehler in "Solid State Physics", Vol. II , F. Seitz and D. Turnbull, Ed., Academic Press Inc., New York, N. Y., 1956, p. 305.

49. H. Müller, J. Inorg. Nucl. Chem., 27, 1745 (1965).

50. J. A. Cairns and S. J. Thomson, J. Inorg. Nucl. Chem. Lett., 3, 107 (1967).

51. R. H. Silsbee, J. Appl. Phys., 28, 1246 (1957).

52. C. Lehmann and G. Leibfried, ibid., 34, 2821 (1963).

53. M. T. Robinson, D. K. Holmes, and O. S. Oen, Bull. Amer. Phys. Soc., 2, 171 (1962).

54. M. T. Robinson, D. K. Holmes, and O. S. Oen, Appl. Phys. Letters, 2, 30 (1963).

55. A. Seeger, Symposium on Radiation Damage in Solids and Reactor Materials, I, IAEA, Vienna, (1962) 101.

56. A. G. Maddock, F. E. Treloar, and J. I. Vargas, Trans. Faraday Soc., 59, 924 (1963).

57. T. Andersen and A. G. Maddock, ibid., 59, 2362 (1963).

58. S. M. Milenkovic and A. G. Maddock, Radiochim. Acta, 8, 222 (1967).

59. D. J. Apers andA. G. Maddock, Trans. Faraday Soc., 56, 498 (1960).

60. A. G. Maddock, M. M. de Maine, and K. Taugbol, Disc. Faraday Soc., 23, 211 (1957).

61. G. Harbottle and N. Sutin, in "Advances in Inorganic Chemistry and Radiochemistry", Vol. 1, Emeleus and Sharpe Ed., Academic Press Inc., New York, N. Y., 1959, p. 267.

62. P. D. Johnson and F. E. Williams, Phys. Rev., 117, 964 (1960).

63. J. Shankar, A. Nath, and V. G. Thomas, J. Inorg. Nucl. Chem., 30, 1361 (1968).

64. K. A. Rao and A. Nath, Radiochim. Acta, 5, 162 (1966).

65. T. Andersen and K. Olesen, Trans. Faraday Soc., 61, 781 (1965).

66. I. McC. Torrens and L. T. Chadderton, Phys. Rev., 159, 671 (1967).

67. G. Harbottle, Conf. Interam. Radioquim., 1st, Montevideo, 1963, p. 261.

68. J. Shankar, K. S. Venkateswarlu, and A. Nath, I, IAEA, Vienna, (1962), p. 309.

69. A. G. Maddock, and M. M. de Maine, Can. J. Chem., 34, 275 (1956).

70. J. Bass and D. Lazarus, J. Phys. Chem. Solids, 23, 1820 (1962).

71. J. S. Butterworth and I. G. Campbell, Trans. Faraday Soc., 59, 2618 (1963).

72. Z. Gyulai, Zeit. Physik, 33, 251 (1925).

73. W. Herr, Z. Electrochemie, 56, 911 (1952).

74. R. F. C. Claridge and A. G. Maddock, Trans. Faraday Soc., 57, 1392 (1961).

75. L. Arizmendi and A. G. Maddock, J. Inorg. Nucl. Chem., 17, 191 (1961).

76. N. Getoff, Radiochim. Acta, 1, 49 (1963).

77. P. Sue", and R. Caillat, Compt. Rend., 230, 1884 (1950).

78. C. J. Delbecq, Z. Phys., 171, 560 (1963).

79. J. H. Crawford, Phys. Rev. Lett., 12, 28 (1964).

80. R. R. Williams, J. Phys. Coll. Chem., 52, 603 (1948).

81. J. W. Cobble and G. E. Boyd, J. Amer. Chem. Soc., 74, 1282 (1952).

82. G. Harbottle, J. Chem. Phys., 22, 1083 (1954).

83. T. Andersen and A. G. Maddock, Trans. Faraday Soc., 59, 1641 (1963).

84. T. Andersen, ibid., 59, 2625 (1963).

85. V. Kacena and A. G. Maddock, Proc. Symposium on Chemical Effects of Nuclear Transformations, II, IAEA, Vienna, (1965), p. 255.

86. J. H. Schulman and W. D. Compton,"Color Centers in Solids", Pergamon Press, Macmillan Co., New York, N. Y., 1962, p. 3, 158.

87. T. Andersen, H. E. Lundager Madsen and K. Olesen, Trans. Faraday Soc., 62, 2409 (1966).

88. R. E. Howard and R. Smoluchowski, Phys. Rev., 116, 314 (1959).

89. L. T. Chadderton, "Radiation Damage in Crystals", John Wiley and Sons, Inc., New York, N. Y., 1965, p.1.

90. E. Fermi, Nature, 133, 898 (1934).

91. E. Fermi, E. Amaldi, O. D'Agostino, F. Resetti, and E. Segre, Proc. Roy. Soc. (London), A, 146, 483 (1934).

92. E. Pollard, Phys. Rev., 57, 1086A (1940).

93. R. C. Allen and W. Rall, Phys. Rev., 81, 60 (1951).

94. B. B. Kinsey, G. A. Bartholomev, and W. H. Walker, Phys. Rev., 85, 1012 (1952).

95. H. Fahlenbrach, Z. Physik, 96, 1503 (1935).

96. M. L. Pool, Physica, 18, 1304 (1952).

97. N. Baron and B. L. Cohen, Phys. Rev., 129, 2636 (1963).

98. R. Sagane, Phys. Rev., 50, 1141 (1936).

99. P. M. Endt and J. C. Kluyver, Revs. Mod. Phys., 26, 95 (1954).

100. R. B. Holtzman and N. Sugarman, Phys. Rev., 87, 633 (1952).

101. H. Adler, P. Huber, and W. Hälg, Helv. Phys. Acta, 26, 349,427)1953).

102. B. H. Levkovskij, Zh. Eksp. Teor. Fiz., 45, 305 (1963).

103. E. B. Paul and R. L. Clarke, Can. J. Phys., 31, 267 (1953).

104. R. S. Scalan and R. W. Fink, Nucl. Phys., 9, 334 (1959).

105. W. Kunz and J. Schintlmeister, "Tabellen der Atomkerne", Teil 1, Akademie-Verlag, Berlin, (1958), p. 84.

106. J. N. Wilson, J. Amer. Chem. Soc., 60, 2697 (1938).

107. V. D. Jonin, A. F. Lekovnikon, M. B. Neiman, and A. N. Nesmeyanov, Dokl. Akad. Nauk., SSSR, 67, 463 (1949).

108. A. I. Brodskii, D. N. Strazhesko, and L. Chervgatsova, ibid., 75, 823 (1950).

109. R. T. Jones and E. H. Swift, Anal. Chem., 25, 1272 (1953).

110. A. Schwicker, Z. Anal. Chem., 110, 161 (1937).

111. I. M. Kolthoff and R. Belcher, "Volumetric Analysis", III, Interscience Publishers, Inc., New York, N. Y., 1957, p. 528.

112. M. Merrington and C. M. Thompson, Biometrika, 33, 75 (1943).

113. A. M. Mood, "Introduction to the Theory of Statistics", McGraw-Hill Co., New York, N. Y., 1950,

114. "Handbook of Tables for Probability and Statistics", The Chemical Rubber Co., Cleveland, Ohio, 1968, p. 304.

115. J. J. Markham, F-Centers in Alkali Halides, "Solid State Physics", F. Seitz and D. Turnbull Ed., Academic Press, New York, N. Y., 1966, p. 5.

PART TWO

HOT ATOM CHEMISTRY OF ^{32}P IN SILICA AND SODIUM SILICATES

I. INTRODUCTION

A. Historical Background

The hot atom chemistry of ^{32}P was first studied by Libby[1] in 1940. Since that time a large number of investigations of the reactions of recoil ^{32}P produced by various means in various systems have been carried out.[2-13] In some of the early experiments, conditions were not well controlled, but this situation has been improved in more recent work.

In the original work by Libby[1], room temperature irradiation of solid sodium phosphate and phosphoric acid solutions with thermal neutrons from a 200 mg Ra-Be source yielded ~50% of the ^{32}P in a form which could be crystallized as orthophosphate. The remainder of the ^{32}P remained in solution and was assumed to be in one or more reduced oxidation states. To explain this Libby proposed that the fraction of ^{32}P in the reduced states represented the fraction of events which resulted in P-O bond rupture; the orthophosphate fraction represented failure to bond rupture by the recoil ^{32}P.

Later Soto, Sellers and Strain[2,3] irradiated crystalline sodium orthophosphate, sodium phosphite and sodium hypophosphite in evacuated quartz tubes at a reactor under a neutron flux of 10^{13} n/cm^2/sec. With Na_2HPO_4 they obtained (one hundred percent) retention* and attributed this to a lack of any bond rupture, while with Na_2HPO_3 and

*Retention may be defined as the percent of activity recovered in the parent form on dissolution of the irradiated material.

NaH_2PO_2 they obtained large amounts of a variety of active products.

Harbottle and Lindner[4] made an extensive study of ^{32}P recoil reactions in crystalline systems as a function of radiation and thermal environment; i.e., temperature of bombardment, flux, neutron to gamma ratio, and annealing conditions. They concluded that bond rupture does occur and explained the presence of reduced as well as the oxidized states in their experiments by bond rupture and local recombination.

In the above experiments ^{32}P was produced by the $^{31}P(n,\gamma)^{32}P$ reaction. The $^{32}S(n,p)^{32}P$[5] and the $^{35}Cl(n,\alpha)^{32}P$ reaction in alkali chlorides have also been studied.[6-13]

The chemical effects of beta decay have been studied in a number of systems.[14] Hsiung and Gordus determined the bond rupture as a result of beta decay of ^{14}C and ^{3}T in some organic compounds. Glentworth and Wiseall investigated the effects of beta-decay of a lanthanide atom, Ce, complexed with amino-polycarboxylic acid chelating ligands.[14] The annealing behavior of ^{131}I in neutron irradiated TeO_2 was studied by Jacimovic, Stevovic and Veljkovic. It has also been possible to synthesize a molecule by a beta decay process. $^{99m}Tc(C_6H_6)_2^+$ was obtained by the decay of ^{99}Mo in the compound $^{99}Mo\ (C_6H_6)_2$. In all cases studied, beta decay leads to bond rupture in some appreciable amounts.

B. Statement of the Problem

Although the hot atom chemistry of ^{32}P produced by the reactions $^{31}P(n,\gamma)^{32}P$, $^{35}Cl(n,\alpha)^{32}P$ and $^{32}S(n,p)^{32}P$ have been investigated, no report on the chemical effects of the $^{32}Si \xrightarrow{\beta^-} {}^{32}P$ reaction has been published. It seemed of particular interest to study the chemical effects of this

reaction for several reasons.

First, ^{32}P is produced by the decay of ^{32}Si, so that the ^{32}P atoms formed find themselves not in an environment made up of other P and O atoms, but in an environment of Si and O atoms. Second, it seemed of interest to compare the results here with those obtained on other ^{32}P systems. Third, it would also be possible to study the effect of crystal structure on the distribution of the oxidation states by the use of SiO_2, Na_2SiO_3 and Na_4SiO_4. Fourth, the system $^{32}Si - ^{32}P - ^{32}S$ provides a unique opportunity to study the effects of beta decay in the absence of gamma radiation.

At the outset it was realized that the amount of ^{32}P which could be produced for these studies was very small and that determination of the distribution in the various oxidation states would be difficult. But in view of previous work on the $^{30}Si(t,p)^{32}Si$ reaction[15,16] and by the use of 90% enriched ^{6}Li in a lithium-silicon alloy and of low-level counting techniques it was hoped that the investigation would prove feasible. The potential significance of the results seemed to justify the risks and efforts involved.

II. GENERAL CONSIDERATIONS

This section was treated at some length in the first part of this thesis. For the following sections please refer to the indicated pages: Nuclear Reactions as a Source of Energetic Atoms (pp. 5-10), Chemical Behavior of Energetic Atoms (pp. 10-23), and Isotopic Exchange Between Phosphorus Oxyanions (pp. 40-41).

A. Silicon Dioxide and Silicates

1. Atomic Arrangement

Silicon dioxide and silicates are in an intermediary position between ionic-inorganic and covalent-organic compounds in their physicochemical characteristics. The binding mechanism in the molecular unit, SiO_2, is the tetrahedral unit coordination group, SiO_4, which has a tendency toward complex polymerization into chains, networks, and frameworks. Sharing of two oxygen atoms per SiO_4 group yields a chain, three oxygen atoms a sheet, and four oxygen atoms a three-dimensional network. The oxide ion is so much larger than the Si^{4+} ion that the four oxygens of an SiO_4 unit are in mutual contact and the silicon ion rests in a tetrahedral hole.[17]

2. Crystal Structure

Silicon dioxide occurs in several crystallographic forms. In all of them silicon is tetrahedrally surrounded by and coordinated to four oxygen atoms by single bonds having considerable ionic character. The difference between the three main types of SiO_2; quartz, tridymite, and cristobalite is a result of variations of frameworks, the basic

tetrahedral pattern being the same.[17]

In metasilicates, SiO_4 tetrahedra form single chains in which each tetrahedron shares two of its oxygen atoms with two other tetrahedra. In such a chain the composition is $(SiO_3^{2-})_n$. The SiO_4 tetrahedra can be arranged in various ways to form chains, depending on the number of repeat units, occurring in the chain.[18] The crystal structure of anhydrous Na_2SiO_3 was determined by Grund and Pizy.[19] Silicon and oxygen atoms form chains of $[Si_2O_6]_\infty^{4-}$ similar to those in pyroxenes, which have 2-repeat unit single chains, Figure 1. The chains are linked through sodium atoms always crystallographically coordinated with five oxygen atoms.

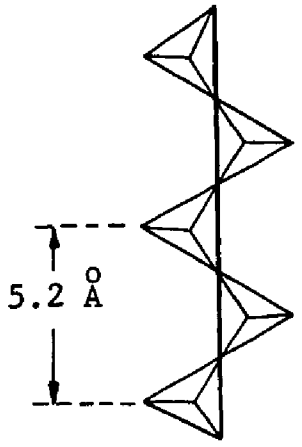

Figure 1

Pyroxene: two repeat unit chain

In ortho-silicates there are simple discrete ortho-silicate, SiO_4, anions.[18] The associated cations are co-ordinated with the oxygen atoms. Various structures are found depending on the coordination number of the cation. The metal oxygen bonds are probably more ionic than the Si-O

bonds; however, there is some covalent character to them. These substances are not ionic in the sense $[M^{2+}]_2[SiO_4^{4-}]$, but rather lie somewhere between this extreme and the opposite extreme of infinite giant molecules.[18] The crystal structure of Na_4SiO_4 has not been reported, but it should be similar to other ortho-silicates and should have separate SiO_4 tetrahedra connected to sodium ions through oxygen atoms.

B. Some Properties of ^{32}Si

1. Production

Search for evidence for the existence of heavier isotopes of Si started as early as 1934. Photometric studies by McKellar[20] showed only ^{28}Si, ^{29}Si and ^{30}Si to be naturally occurring. Later Ney and McQueen[21] measured the relative abundance of the Si isotopes by a Nier type mass spectrometer. The percentages are: 92.24 ± 0.10 for ^{28}Si, 4.69 ± 0.05 for ^{29}Si and 3.07 ± 0.05 for ^{30}Si. None of the rare isotopes was reported. An upper limit of abundance of ^{32}Si was set to be 1/50,000 relative to ^{28}Si.

Since then artificial production of ^{32}Si has been done by a number of people using different procedures. The first synthesis is attributed to Lindner.[22,23] He used $^{37}Cl(p,\alpha 2p)^{32}Si$ reaction, NaCl being the target material. NaCl was bombarded with 340 Mev protons from the Berkeley 184-inch cyclotron. The nuclear reactions used are $^{30}Si(t,p)^{32}Si$[15,16,24], $^{30}Si(n,\gamma)^{31}Si(n,\gamma)^{32}Si$[25] and $^{32}P(n,p)^{32}Si$.[26] In the present work $^{30}Si(t,p)^{32}Si$ reaction is used. Tritiums are obtained by $^{6}Li(n,\alpha)T$ reaction. Production of ^{32}Si by this method was studied extensively by Jantsch.[15,16]

The effective cross section of this reaction calculated by Jantsch is 0.79-0.31 mb for Li-Si alloys of 10-70% Si content, where tritium atoms have an energy of 2.73 Mev.

The potential barrier for this reaction is 4.32 Mev.

2. Decay Scheme

Silicon-32 decays into ^{32}P by pure negatron emission. The maximum beta energy is about 0.1 Mev. Phosphorus-32 is also radioactive and decays to stable ^{32}S, again by a pure beta emission. The maximum energy for this decay is 1.71 Mev. The half-life of ^{32}Si is estimated to be 700 years and that of ^{32}P 14.3 days. The decay scheme is shown in Figure 2.[26]

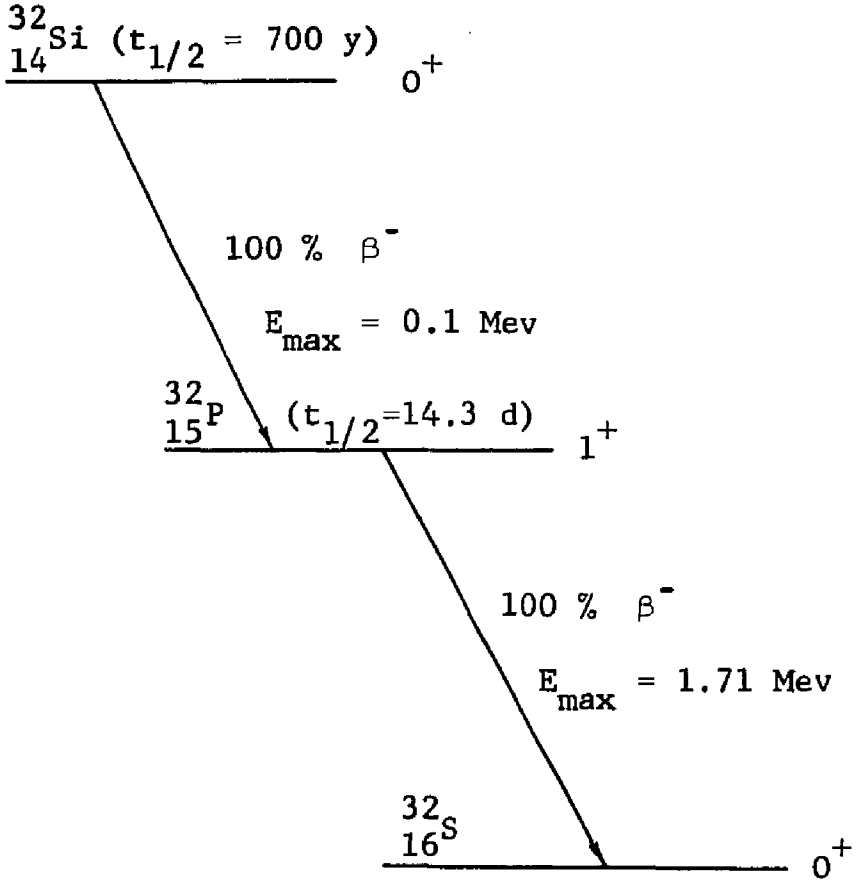

Figure 2

Decay Scheme of ^{32}Si

3. The Growth of ^{32}P

The growth of any radioactive daughter, e.g. ^{32}P, can be calculated as a function of time. $-\frac{dN_1}{dt} = \lambda_1 N_1$ represents the rate of decay of the parent. The daughter is formed at the rate of the parent decay and it decays at the rate $\lambda_2 N_2$.

$$\frac{dN_2}{dt} = \lambda_1 N_1 - \lambda_2 N_2 \quad .$$

When $N_1 = N_1^\circ e^{-\lambda_1 t}$ (where N_1° represents the value of N_1 at $t = o$) is substituted in the above equation:

$$\frac{dN_2}{dt} + \lambda_2 N_2 - \lambda_1 N_1^\circ e^{-\lambda_1 t} = 0 \quad .$$

The equation is solved for N_2,

$$N_2 = \frac{\lambda_1}{\lambda_2 - \lambda_1} N_1^\circ (e^{-\lambda_1 t} - e^{-\lambda_2 t}) + N_2^\circ e^{-\lambda_2 t} \quad ,$$

where the first group of terms shows the growth of daughter from the parent and the decay of these daughter atoms; the last term gives the contribution at any time from the daughter atoms present initially.

Since in this case the parent ^{32}Si has a much longer half-life than the daughter ^{32}P, after a certain time a radioactive equilibrium is reached where the ratio of the disintegration rates of parent and daughter becomesconstant. After t becomes sufficiently large, $e^{-\lambda_2 t}$ is negligible compared with $e^{-\lambda_1 t}$. $N_2^\circ e^{-\lambda_2 t}$ is also negligible, so the equation becomes

$$N_2 = \frac{\lambda_1}{\lambda_2 - \lambda_1} N_1 \quad .$$

This equilibrium is reached after about 30 days in the case of ^{32}Si - ^{32}P decay as shown in Figure 3.

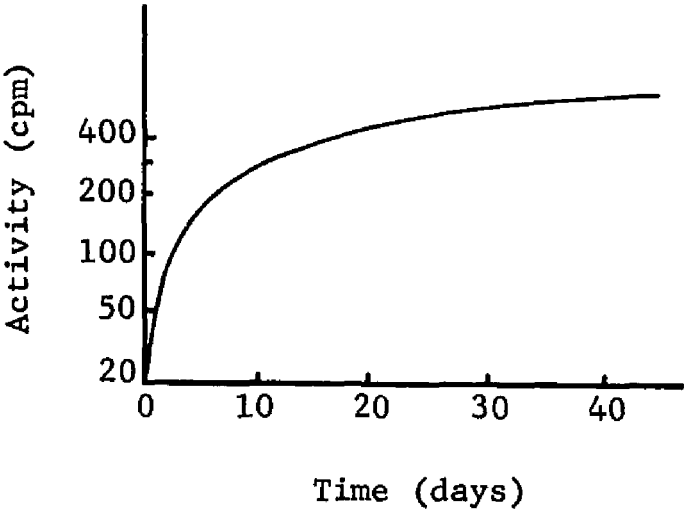

Figure 3

The Growth of the Daughter, ^{32}P

III. EXPERIMENTAL DETAILS

A. Preparation of Samples

Lithium silicide alloys are not commercially available. In this work they were prepared according to the procedure of Klemm and Struck.[27] Ordinary lithium metal used in this reaction was supplied by Fisher Scientific Co. Lithium metal enriched in ^{6}Li (90%) was obtained from Oak Ridge National Laboratory. Silicon was obtained from Fisher Scientific Co.

To carry out the synthesis, 4.65 g of Si and 1.7 g of Li (twice as much Li as Si on a mole basis to give Li_2Si) were weighed and placed in a nickel boat in a dry box filled with argon. The boat was put in a glass tube, stoppered, and then transferred into a tube furnace through which argon flowed at a constant rate. The temperature of the furnace was raised to 530°C and the sample left at this temperature for an hour. The apparatus was left to cool under the flow of argon overnight. The alloy was ground to powder and stored. It was grey in color and appeared to contain no unreacted lithium.

B. Irradiation of Samples

The first batch of Li-Si alloy was prepared with natural Li. One gram quantities were placed in aluminum capsules and were heat-sealed. These samples were irradiated at the U.S. Army Materials and Mechanics Research Center Reactor, Watertown, Mass., for a period of one month. However, the actual irradiation time was less than a month since the reactor did not operate continuously, and part of the time it was operating at reduced power. The neutron flux was about $2 \times 10^{12} n/cm^2/sec$, the gamma flux about 140 Mrads/hr

and the ambient temperature 100°C.

The second batch of Li-Si alloy was prepared with 90% enriched ^{6}Li isotope. In this case, 0.5 g samples were vacuum-sealed in quartz tubes, drawn into a capillary at one end (Figure 4).

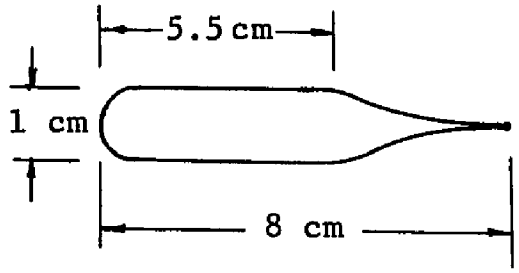

Figure 4

A Sample Quartz Tube

Some of them were sent to the reactor at M.I.T., Cambridge, Mass., and some to the reactor at Brookhaven National Laboratory, Upton, L.I., N. Y.

Samples sent to the M.I.T. reactor were reduced to 0.1 g each. Although the nominal neutron flux was 2×10^{13} $n/cm^2/sec$, it was somewhat less than this value where the samples were irradiated.

Those sent to the Brookhaven reactor were further wrapped with quartz glass wool and placed in larger quartz tubes which were again vacuum-sealed. They were irradiated for 46 hours. The neutron flux was $1 \times 10^{13} n/cm^2/sec$. Some experimental difficulties were encountered at the Brookhaven reactor. The first and second samples apparently exploded because of the large heat build-up. Successful irradiations were obtained only by removing the sample tubes from the outer jackets and wrapping them in aluminum tape and irradiating in an air-cooled column.

All samples were kept at room temperature for at least a week pending the subsequent treatment.

C. Post Irradiation Treatment of the Samples

The samples irradiated in aluminum capsules were opened under a hood vented directly to the outdoors.

Those irradiated in quartz tubes were treated in the following way to prevent the escape into the atmosphere of tritium (produced by $^{6}Li(n,\alpha)T$ reaction) and to control the violent decomposition reaction of Li_2Si in sodium hydroxide solution.

The apparatus was set up as shown in Figure 5. The sample tube was put in flask B together with a magnetic stirring bar. The pressure equalizing funnel, A, contained 5 M NaOH solution. A Dewar flask, C, containing dry ice in acetone was used as a trap. Another round bottom flask, D, contained nitrobenzene which, in the presence of a catalyst of palladium on charcoal, reacted with evolved H_2 gas containing trace amounts of tritium. The H_2 gas was generated by the reaction:

$$Li_2Si + 4H_2O \rightarrow 2\ LiOH + (SiO_2)_x + 3H_2\uparrow$$

Initially the system was disconnected at E. Nitrogen gas was flowed through it for an hour to displace the air. Then the apparatus was connected and the flow of nitrogen stopped.

In the closed system the sample tube was broken open by dropping the Teflon-coated stirring bar on it with the help of a horseshoe magnet manipulated from outside. The sodium hydroxide solution was allowed to drip on the sample, which decomposed slowly, giving off H_2 gas which bubbled through nitrobenzene. As the pressure of H_2 in the system

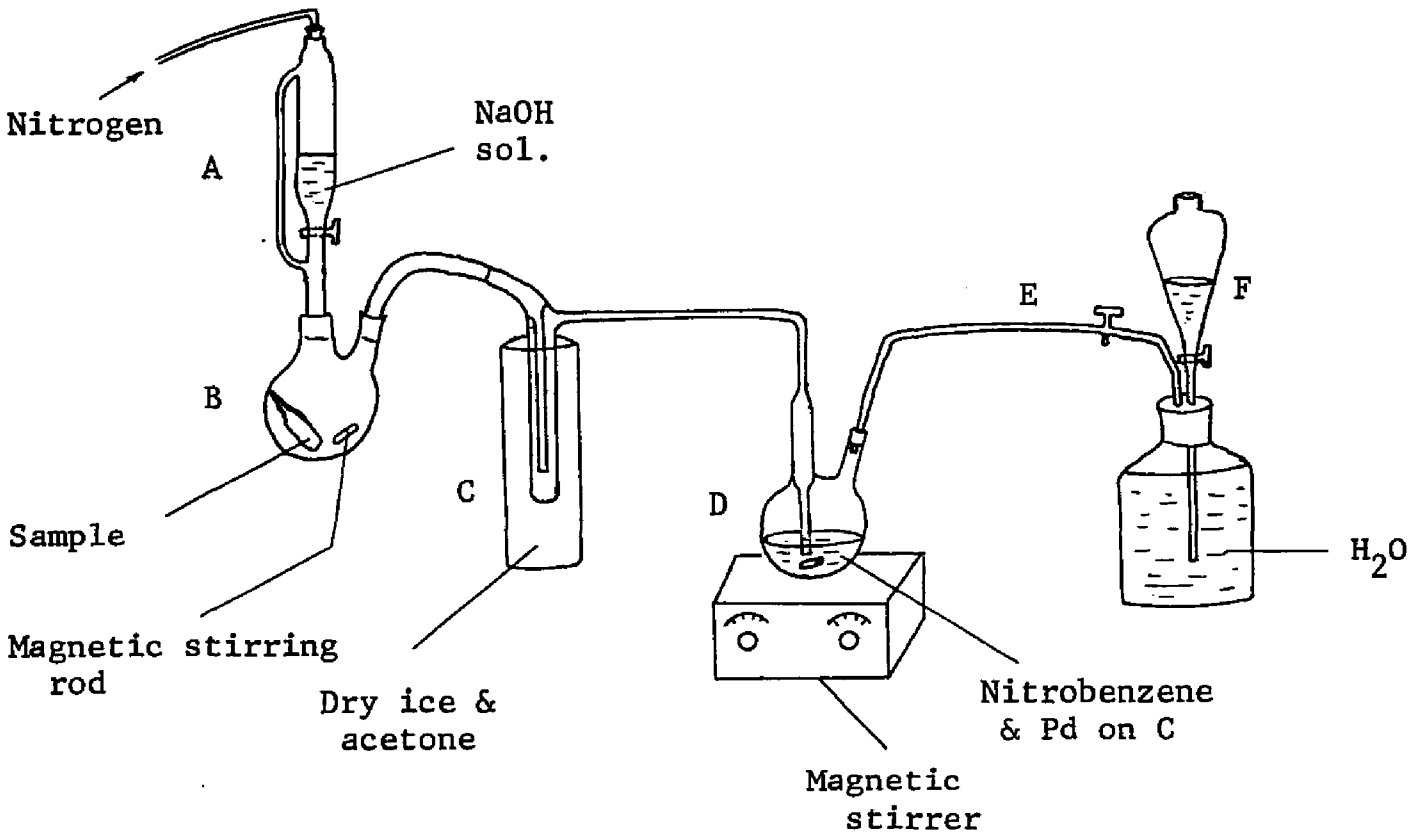

Figure 5

The Apparatus Used for the Decomposition of
Radioactive Li-Si Alloys Under Closed System

built up, the water level in F rose. The rate of addition of NaOH solution was regulated so that the production of H_2 was about the same as its rate of reaction with nitrobenzene, so the water level in F remained the same. Decomposition required two days to complete. When the evolution of H_2 stopped, flask D was disconnected, stoppered and saved.

Flask B was heated by a heating mantle and H_2O was distilled over into trap C. A grayish, white solid was left in B. This was scraped off and dissolved in hot concentrated 10 M NaOH solution. The solution was filtered to remove the impurities. To the clear solution 20 ml 7 M H_2SO_4 was added. A gelatinous precipitate formed. The solution was then evaporated to dryness, the residue transferred into a porcelain crucible, and ignited. Impurities discoloring SiO_2 evaporated, leaving behind a white solid, containing Na_2SO_4, Li_2SO_4 and SiO_2. Upon the addition of 100 ml of distilled water the first two compounds dissolved. Silicon dioxide was filtered, washed and ignited again to drive off any moisture. A fluffy white solid was obtained. X-ray analysis showed it to be amorphous (no identifiable lines).

Flask D contained nitrobenzene, catalyst palladium on charcoal, and some aniline formed during the reaction of H_2 with nitrobenzene.[28]

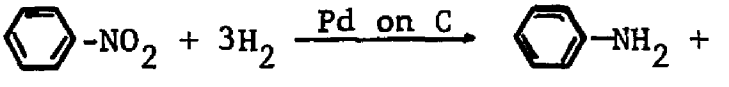

It also contained trace amounts of 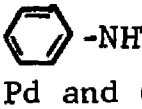 -NHT and/or 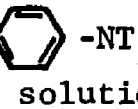 $-NT_2$. This mixture was filtered to remove Pd and C. To the solution more aniline was added and then HCl gas was bubbled through the solution. Aniline hydrochloride, a white solid, precipitates out. It was filtered and washed with ether, dried and stored in a closed bottle.[29]

D. Preparation of ^{32}Si - Labelled Na_2SiO_3

Silicon dioxide obtained above was further used in the preparation of Na_2SiO_3. Silicon dioxide, 0.8860 g, was mixed with 1.5623 g Na_2CO_3. The mixture was fused in a platinum crucible at 1150°C for two hours. The melt was then brought to 700°C and left to crystallize for four days. Sodium meta silicate formed according to the reaction:[30]

$$SiO_2 + Na_2CO_3 \rightarrow Na_2SiO_3 + CO_2\uparrow$$

X-ray powder diffraction patterns of the crystalline product were taken and the d-values compared to the ASTM values, confirming the existence of sodium meta silicate. The experimental and standard d-values are listed in Table I.

E. Preparation of ^{32}Si - Labelled Na_4SiO_4

Previously prepared SiO_2, 0.2160 g, was mixed with 0.7630 g Na_2CO_3 in a platinum crucible. The mixture was heated to 1100°C and left to crystallize at 1040-1060°C for 24 hours, forming Na_4SiO_4 according to the reaction:[31]

$$SiO_2 + 2Na_2CO_3 \rightarrow Na_4SiO_4 + 2CO_2\uparrow$$

A white crystalline product was obtained. Part of it was powdered, and an x-ray powder-pattern was taken. However, there are no listed d-values for this compound. To confirm the presence of sodium ortho-silicate, commercially available product was bought, and the x-ray pattern was taken. The d-values for the commercial and the synthesized compounds matched very well. The data are shown in Table II.

Table I

Powder Pattern of Na_2SiO_3

Experimental		Standard	
d-value	Relative Intensity	d-value	Relative
5.2771	m	5.3	20
3.5900	m	3.56	20
3.0582	vvs	3.04	100
2.6069	vs	2.57	48
2.4295	s	2.40	64
2.3094	vvw		
1.9811	vw	1.98	9
1.8879	s	1.88	28
1.8309	vw	1.83	9
1.7460	s	1.75	40
1.6420	vvw		
1.5325	w	1.53	5
1.4467	w	1.45	9
1.4231	s	1.42	40
1.2521	vvw	1.15	3
1.1220	s	1.11	9
		1.03	2
		0.99	2
		0.93	2

Table II

Powder Pattern of Na_4SiO_4

Experimental		Commercial Product	
d-value	Relative Intensity	d-value	Relative Intensity
5.7535	vvw		
5.2771	w	5.2771	m
4.7199	m		
3.7385	vw		
3.6187	w	3.5617	w
3.0379	s	3.0582	vvs
2.5923	vvs	2.5779	s
2.3559	vs	2.4044	vs
2.2539	vvw		
2.1910	vw	2.1809	vvw
2.1127	vvw		
1.8879	m	1.9028	s
1.7648	m	1.7585	s
1.5418	vvw	1.5371	vvw
1.4839	vvw		
1.4547	vw		
1.4192	m	1.4231	vs
1.1178	w		

F. Storage Conditions

To determine the effect of temperature on the reactions and ultimate states of the ^{32}P produced by the decay of ^{32}Si, aliquots of the prepared samples were sealed in vials and maintained at -196°, -78°, 0°, 20-25°, and 100°C for at least one month prior to analysis. During this time ^{32}P radioactivity grows to about 75% of its equilibrium value. About 100 mg SiO_2, 200 mg Na_2SiO_3, and 300 mg Na_4SiO_4 were taken, so that approximately equal amounts of ^{32}P would eventually appear in each aliquot.

G. Analysis of the Samples

The detailed description of this method with mounting and counting techniques was given in the first part of this thesis. Only a general outline will be given in this section.

The samples stored at various temperatures were dissolved in carrier solutions (0.2 mmole in each of $Na_2HPO_4 \cdot 12H_2O$, $Na_2HPO_3 \cdot 5H_2O$, $NaH_2PO_2 \cdot H_2O$ and $Na_4P_2O_7 \cdot 10H_2O$ to give 50 mg of $NH_4MgPO_4 \cdot 6H_2O$ for each). From this solution phosphate alone was precipitated as $NH_4MgPO_4 \cdot 6H_2O$ in the presence of the others. It was filtered, washed and dried before counting. The filtrate was saved. $P_2O_7^{4-}$ ion was converted to PO_4^{3-} by adding a few ml of 50% HNO_3 to the filtrate and heating. Again PO_4^{3-} was precipitated as $NH_4MgPO_4 \cdot 6H_2O$. The PO_3^{3-} ions, left in the filtrate which were oxidized with iodine solution to PO_4^{3-} and the PO_2^{3-} ions were oxidized with H_2O_2 solution and both precipitated as before.

The same solution was used to separate the different oxidation states successively. In this way all activity due to ^{32}P was recovered.

H. Radioactivity Measurements

All four precipitates were mounted on metal discs using a chimney-funnel set-up (described in the first part, pp. 47-49) and the radioactivity counted as described then.

Each sample was placed in a copper sample pan and then transferred into a specially constructed plastic planchet holder. An aluminum absorber of 39.1 mg/cm^2 thickness was placed between the sample and the detector to eliminate any foreign activity. Each sample was counted long enough to accumulate 1000 counts. The background was counted with the absorber on before the sample count, using a non-radioactive $NH_4MgPO_4 \cdot 6H_2O$ prepared in exactly the same way as the sample. Corrections were made for the background.

It was not necessary to make coincidence corrections. The instrument has a resolving time of 0.5 μs equivalent at 10^6 cpm, using live timing. In this work no count rate exceeded 60 cpm.

IV. RESULTS AND DISCUSSION

Typical activities obtained as a result of ^{32}P decay in each of the four oxidation states are given in Table III. The SiO_2 in Table III was kept at 0°C for more than a month before analysis and the Na_2SiO_3 at 20-25°C for about the same length of time. As we see from the table the activities are not much higher than the background. The net count is lower than 1 cpm in most of the cases. Under these circumstances to calculate the percentage activity in each oxidation state becomes meaningless since the statistical errors are often greater than the activity itself. Some of the activities obtained were even lower than the values listed below.

The results indicate that not enough activity was obtained either to make reasonable comparison of the distribution of the activity among the oxidation states of phosphorus or to attribute this activity to ^{32}P, since it is impossible to take the decay curve of such a sample. However, by using a 0.5 g sample of Li-Si, isolating the total ^{32}P activity as $NH_4MgPO_4 \cdot 6H_2O$, the total initial activity obtained was 59 cpm. The decay curve shown in Figure 6 clearly indicates the presence of ^{32}P. The experimental half-life obtained from the curve is $t_{1/2}$ = 14.25 days. The theoretical half-life is 14.295 days.[26]

The reasons for the low ^{32}P activity obtained seem more practical than theoretical. According to Jantsch[16] the effective cross section for the $^{30}Si(t,p)^{32}Si$ reaction is of the order of 0.5 mb. Thus with 1 g Li-Si samples containing 70 mole percent ordinary silicon and 30 mole percent enriched lithium (90% ^{6}Li), a 48 hour irradiation at a neutron flux of

Table III

Distribution of ^{32}P Activity Between
Four Phosphorus Oxyanions

Sample	Fraction	Gross cpm	Bkgd cpm	Net cpm
SiO_2	$^{32}PO_4^{3-}$	2.47 ± 0.08	1.69 ± 0.18	0.78 ± 0.26
"	$^{32}P_2O_7^{3-}$	2.18 ± 0.07	1.69 ± 0.18	0.49 ± 0.25
"	$^{32}PO_3^{3-}$	2.14 ± 0.07	1.60 ± 0.18	0.54 ± 0.25
"	$^{32}PO_2^{3-}$	1.77 ± 0.06	1.60 ± 0.18	0.17 ± 0.24
Na_2SiO_3	$^{32}PO_4^{3-}$	2.90 ± 0.09	1.48 ± 0.17	1.42 ± 0.26
"	$^{32}P_2O_7^{3-}$	3.00 ± 0.09	1.48 ± 0.17	1.52 ± 0.26
"	$^{32}PO_3^{3-}$	1.68 ± 0.05	1.48 ± 0.17	0.20 ± 0.22
"	$^{32}PO_2^{3-}$	2.28 ± 0.07	1.48 ± 0.17	0.80 ± 0.24

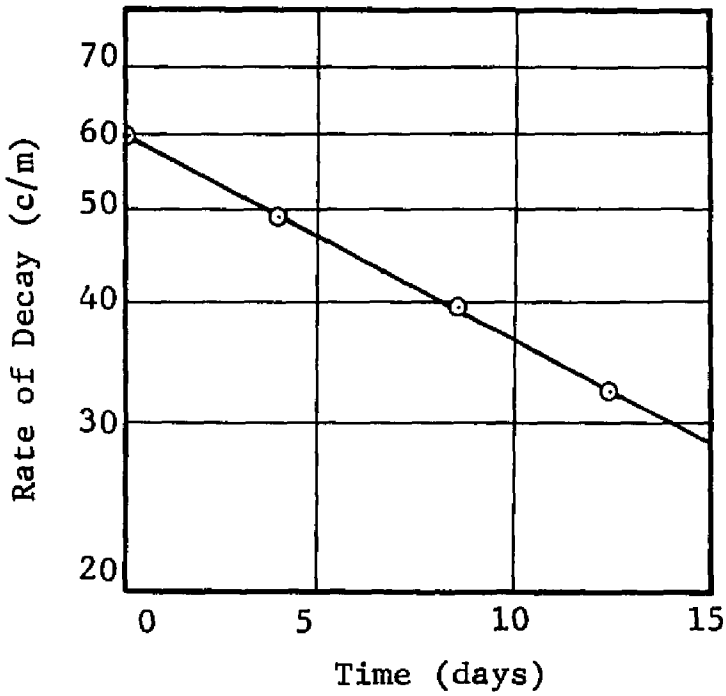

Figure 6

Experimental Decay Curve of ^{32}P

1×10^{12} n/cm^2/sec should yield an equilibrium ^{32}P radioactivity of 135 dpm. Longer irradiations, higher flux, larger samples, and/or the use of enriched silicon would increase this value.

The use of more optimum conditions was prohibited by a number of considerations:

1) Because of the large amount of heat generated by the $^6Li(n,\alpha)T$ reaction, sample sizes were restricted to not more than 1 gram in the Watertown reactor, not more than 0.5 gram in the Brookhaven reactor, and not more than 0.1 gram in the M.I.T. reactor.

2) In none of the irradiation positions used was the available neutron flux significantly greater than 1×10^{12} n/cm^2/sec, nor were other positions with higher fluxes in these reactors available.

3) Longer irradiations were prohibited either for financial reasons or by other reactor requirements.

4) At the time of these experiments, the by-product materials license held by the University of New Hampshire permitted possession of no more than 2.1 curies of tritium at any one time.

5) At the time of these experiments, no source of ^{30}Si-enriched silicon was known.

Because of the extremely low ^{32}P radioactivity obtained under the permitted irradiation conditions and because of the above considerations, it was concluded that these experiments were not feasible at this time, and further work was abandoned.

V. SUGGESTIONS FOR FURTHER WORK

Hot atom chemistry of ^{32}P in this system is very interesting from the standpoint of the following considerations. In all the systems studied so far ^{32}P has been produced by a nuclear reaction directly in the particular compound under study. In this system ^{32}P is produced not as a result of a nuclear reaction, but as a result of the radioactive decay of ^{32}P.

Radiation effects observed in irradiated crystals and which often obscure or interfere with hot atom reactions would be absent in ^{32}Si-^{32}P system. The irradiated material is Li-Si alloy. The expected radiation effects would be quite large in the alloy itself, since it was irradiated for a long period of time, 2-30 days. However, hot atom chemistry of ^{32}P was studied in SiO_2, Na_2SiO_3 and Na_4SiO_4 crystals. The irradiated material, Li-Si, was decomposed and so the radiation effects were eliminated and the new crystals of SiO_2, Na_2SiO_3 and Na_4SiO_4 were prepared in the pure form.

There has been no attempt so far to investigate the effect of crystal structure; the oxidation state, nature and the size of the cation; and the availability of and the number of oxygens in the crystal on the distribution of the ^{32}P recoils among its various oxidation states. It would be interesting to determine the effect of crystal structure in different silicates. SiO_2 prepared in this work was amorphous with no definite crystal structure. Na_2SiO_3 has a pyroxene type arrangement of silicate tetrahedra in which two oxygen atoms are shared to form a chain and Na_4SiO_4 has discrete SiO_4 tetrahedra. Here, the effect of availability of oxygen

atoms would be interdependent with the effect of crystal structure. The domination of PO_2^{3-} ion in SiO_2, PO_3^{3-} ion in Na_2SiO_3 and PO_4^{3-} ion in Na_4SiO_4 would be expected. There might also be an effect due to the absence of a cation in SiO_2 or presence of Na^+ ions in Na_2SiO_3 and Na_4SiO_4 crystals.

There is no doubt that ^{32}Si and hence ^{32}P is obtained by the method used here, but not enough of it is produced for the purposes intended. The obvious requirement for further work is to obtain more ^{32}Si.

If arrangements can be made for doing so, implementation of the conditions mentioned above should result in the desired amount of ^{32}Si. However, as indicated, various practical difficulties would have to be overcome.

The possibility of using other sources of ^{32}Si, such as the $^{30}Si(2n,\gamma)^{32}Si$, $^{32}P(n,p)^{32}Si$ reactions should be investigated.

Since nuclear explosions produced tremendous neutron fluxes for short times, it might be possible to obtain ^{32}Si produced by the double neutron capture of ^{30}Si in sand at nuclear test sites. Here, of course, the specific activity would be very low, and other radioactivities might interfere.

VI. LIST OF REFERENCES

1. W. F. Libby, J. Amer. Chem. Soc., 62, 1936 (1940).

2. T. R. Sato, P. A. Sellers, and H. H. Strain, J. Inorg. Nucl. Chem., 5, 31 (1957).

3. T. R. Sato, P. A. Sellers, and H. H. Strain, ibid., 11, 84 (1959).

4. G. Harbottle and L. Lindner, ibid., 15, 386 (1960).

5. A. Adams and I. G. Campbell, Trans. Faraday Soc., 59, 2001 (1963).

6. A. H. W. Aten, Jr., Rec. Trav. Chim. Pays-Bas, 61, 467 (1942).

7. A. H. W. Aten, Jr., Phys. Rev., 71, 641 (1947).

8. R. Caillat and P. Sue II, Compt. Rend., 230, 1666 (1950).

9. L. Lindner, Ph. D. Thesis, University of Amsterdam, 1958.

10. T. A. Carlsen and W. S. Koski, J. Chem. Phys., 23, 1596 (1955).

11. J. S. Butterworth and I. G. Campbell, Nature, 196, 982 (1962).

12. J. Cifka, Proc. Symposium on Chemical Effects of Nuclear Transformations, II, IAEA, Vienna, (1965), p. 71.

13. J. L. Babtista, G. W. A. Newton, and V. J. Robinson, Trans. Faraday Soc., 64, 456 (1968).

14. Proc. Symposium on Chemical Effects Associated with Nuclear Reactions and Radiative Transformations, II, IAEA, Vienna, (1965), p. 461-546.

15. K. Jantsch, Kernenergie, 4, 846 (1961).

16. K. Jantsch, ibid., 9, 127 (1966).

17. W. Eitel, "Physical Chemistry of the Silicates", University of Chicago Press, Chicago, 1954, p. 11.

18. W. Eitel, "Silicate Science", Vol. I, Academic Press Inc., New York, N. Y., 1964, p. 11, 52.

19. A. Grund and M. Pizy, Acta Cryst., 5, 837 (1952).

20. A. McKellar, Phys. Rev., 45, 761 (1934).

21. E. P. Ney and J. H. McQueen, Phys. Rev., 69, 41 (1946).

22. M. Lindner, ibid., 89, 1150 (1953).

23. M. Lindner, ibid., 91, 642 (1953).

24. D. Geithoff, Radiochim. Acta, 1, 3 (1962).

25. A. Samuels and A. Turkevich, Phys. Rev., 94, 364 (1954).

26. W. Kunz and J. Schintlmeister, "Tabellen der Atomkerne", Akademie-Verlag, Berlin, 1958, p. 76, 84.

27. W. Klemm and M. Struck, Z. Anorg. Allg. Chem., 278, 117 (1955).

28. H. Kolbe, J. Prakt. Chem., 4, 418 (1871).

29. L. F. Feiser and M. Feiser, "Organic Chemistry", D. C. Heath and Co., Boston, Mass., 1950, p. 636.

30. R. Schwarz, Z. Anorg. Allg. Chem., 126, 62 (1923).

31. A. M. Ginstling and T. P. Fradkina, J. Appl. Chem. U.S.S.R., 25, 1325 (1952).

APPENDIX

Program for Polynomial Regression

Program for Polynomial Regression*

Language: IBM 360 FORTRAN IV

Input: Each set of data cards starts with an identification card.

Indentification card:

Card space	1 - 6	7 - 11	12 - 13	14
Variable		N	M	N PLOT
	Identification	Number of Observations	Highest degree of Polynomial	0

Data Cards were prepared according to the FORMAT (2F 10.6) as follows:

Space	1 - 10	11 - 20
Variable	X(I)	X(J)
	Annealing Time	Percentage

*This program was written by Robert Murphy, graduate student at the University of New Hampshire

IBM OS/360 BASIC FORTRAN IV (E) COMPILATION

```
      DIMENSION X(660),DI(100),D(66),B(10),E(10),SB(10),I(10),
     1XBAR(11),ISTD(11),COE(11),SUMSQ(11),ISAVE(11),ANS(10),P(120)
    1 FORMAT(A4,A2,I5,I2,I1)
    2 FORMAT(2F10.6)
    3 FORMAT(27HIPOLYNOMIAL REGRESSION.....A4,A2/)
    4 FORMAT(23HONUMBER OF OBSERVATIONS,16//)
    5 FORMAT(32HOPOLYNOMIAL REGRESSION OF DEGREE,13)
    6 FORMAT(12HO  INTERCEPT,F15.5 )
    7 FORMAT(26HO REGRESSION COEFFICIENTS/(10E15.5))
    8 FORMAT(1HO/24X,24HANALYSIS OF VARIANCE FOR,14,19H DEGREE
     1POLYNOMIAL/)
    9 FORMAT(1HO,5X,19HSOURCE OF VARIATION,7X,9HDEGREE OF,7X,
     1,6HSUM OF,9X,4HMEAN,10X,1HF,9X,20HIMPROVEMENT IN TERMS/33X,
     2,7HFREEDOM,8X,7HSQUARES,7X,6HSQUARE,7X,5HVALUE,8X,17HOF SUM
     3OF SQUARES)
   10 FORMAT(20HO  DUE TO REGRESSION,12X,16,F17.5,F14.5,F13.5,
     1F20.5)
   11 FORMAT(32H   DEVIATION ABOUT REGRESSION   ,16,F17.5F14.5)
   12 FORMAT(8X,5HTOTAL,19X,16,F17.5///)
   13 FORMAT(17HO  NO IMPROVEMENT)
   14 FORMAT(1HO//27X,18HTABLE OF RESIDUALS//16H OBSERVATION NO.,
     1,5X,7HX VALUE,7X,7HY VALUE,7X,10HY ESTIMATE,7X,8HRESIDUAL/)
   15 FORMAT(1HO,3X,16,F18.5,F14.5,F17.5,F15.5)
  100 READ(1,1) PR,PR1,N,M,NPLOT
      WRITE(3,3)PR,PR1
      WRITE(3,4)N
      L=N*M
      DO 110 I=1,N
      J=L+I
  110 READ(1,2) X(I),X(J)
      CALL GDATA (N,M,X,XBAR,STD,D,SUMSQ)
      MM=M+1
      SUM=0.0
      NT=N-1
      DO 200 I=1,M
      ISAVE(I)=I
      CALL ORDER (MM,D,MM,I,ISAVE,DI,E)
      CALL MINV (DI,I,DET,B,T)
      CALL MULIR (N,I,XBAR,STD,SUMSQ,DI,E,ISAVE,B,SB,T,ANS)
      WRITE(3,5)I
      IF(ANS(7)) 140,130,130
```

```
130 SUMIP=ANS(4)-SUM
    IF(SUMIP) 140,140,150
140 WRITE(3,13)
    GO TO 210
150 WRITE(3,6) ANS(1)
    WRITE(3,7) (B(J),B=1,I)
    WRITE(3,8) I
    WRITE(3,9)
    SUM=ANS(4)
    WRITE(3,10) I,ANS(4),ANS(6),ANS(10),SUMIP
    NI=ANS(8)
    WRITE(3,11) NI,ANS(7),ANS(9)
    WRITE(3,12) NI,SUMSQ(MM)
    COE(1)=ANS(1)
    DO 160 J=1,I
160 COE(J+1)=B(J)
    LA=I
200 CONTINUE
210 IF(NPLOT) 100,100,220
220 NP3=N+N
    DO 230 I=1,N
    NP3=NP3+1
    P(NP3)=COE(1)
    L=I
    DO 230 J=1,N
    P(NP3)=P(NP3)+X(L)*COE(J+1)
230 L=L+N
    N2=N
    L=N*M
    DO 240 I=1,N
    P(I)=X(I)
    N2=N2+1
    L=L+1
240 P(N2)=X(L)
    WRITE(3,3)PR,PR1
    WRITE(3,5)LA
    WRITE(3,14)
    NP2=N
    NP3=N+N
    DO 250 I=1,N
    NP2=NP2+1
    NP3=NP3+1
    RESID=P(NP2)-P(NP3)
250 WRITE(3,15) I,P(I),P(NP2),P(NP3),RESID
    CALL PLOT (LA,P,N,3,0,1)
    GO TO 100
    END
```